



Isolation and Characterization of a Novel Temperate *Escherichia coli* Bacteriophage, Kapi1, Which Modifies the O-Antigen and Contributes to the Competitiveness of Its Host during Colonization of the Murine Gastrointestinal Tract

 Kat Pick,^a Tingting Ju,^b Benjamin P. Willing,^b  Tracy L. Raivio^a

^aDepartment of Biological Sciences, University of Alberta, Edmonton, Alberta, Canada

^bDepartment of Agricultural, Food and Nutritional Science, University of Alberta, Edmonton, Alberta, Canada

ABSTRACT In this study, we describe the isolation and characterization of novel bacteriophage vB_EcoP_Kapi1 (Kapi1) isolated from a strain of commensal *Escherichia coli* inhabiting the gastrointestinal tract of healthy mice. We show that Kapi1 is a temperate phage integrated into tRNA *argW* of strain MP1 and describe its genome annotation and structure. Kapi1 shows limited homology to other characterized prophages but is most similar to the seroconverting phages of *Shigella flexneri* and clusters taxonomically with P22-like phages. The receptor for Kapi1 is the lipopolysaccharide O-antigen, and we further show that Kapi1 alters the structure of its host's O-antigen in multiple ways. Kapi1 displays unstable lysogeny, and we find that the lysogenic state is more stable during growth in simulated intestinal fluid. Furthermore, Kapi1 lysogens have a competitive advantage over their nonlysogenic counterparts both *in vitro* and *in vivo*, suggesting a role for Kapi1 during colonization. We thus report the use of MP1 and Kapi1 as a model system to explore the molecular mechanisms of mammalian colonization by *E. coli* to ask what the role(s) of prophages in this context might be.

IMPORTANCE Although research exploring the microbiome has exploded in recent years, our understanding of the viral component of the microbiome is lagging far behind our understanding of the bacterial component. The vast majority of intestinal bacteria carry prophages integrated into their chromosomes, but most of these bacteriophages remain uncharacterized and unexplored. Here, we isolate and characterize a novel temperate bacteriophage infecting a commensal strain of *Escherichia coli*. We aim to explore the interactions between bacteriophages and their hosts in the context of the gastrointestinal tract, asking what role(s) temperate bacteriophages may play in growth and survival of bacteria in the gut. Understanding the fundamental biology of gut commensal bacteria can inform the development of novel antimicrobial or probiotic strategies for intestinal infections.

KEYWORDS gastrointestinal colonization, lysogen, temperate

Escherichia coli is a Gram-negative bacterium normally inhabiting the lower gastrointestinal (GI) tract of humans and other warm-blooded animals (1). Despite being one of the most widely studied prokaryotic model organisms, there remains an immense complexity to the lifestyle of *E. coli* that we are only beginning to appreciate; one of these layers of complexity is the interactions between *E. coli* and the bacteriophages that infect it. Bacteriophages (or simply phages) exhibit two main lifecycles, lytic and lysogenic. Lytic phages infect and immediately begin replicating within their host, eventually causing cell lysis and releasing progeny phages. Temperate phages replicate through the same lytic cycle but can also display an alternate life cycle, the lysogenic cycle, where the phages can

Editor Matthew R. Chapman, University of Michigan-Ann Arbor

Copyright © 2022 Pick et al. This is an open-access article distributed under the terms of the [Creative Commons Attribution 4.0 International license](https://creativecommons.org/licenses/by/4.0/).

Address correspondence to Tracy L. Raivio, traivio@ualberta.ca.

The authors declare no conflict of interest.

Received 1 November 2021

Accepted 23 December 2021

Published 25 January 2022

integrate into the genome of their host, replicating along with the host chromosome and being disseminated into daughter cells. Once the host cell experiences stress such as DNA damage, the prophage excises from the chromosome and enters the lytic cycle to ensure its own survival (2). Temperate phages have been gaining attention as we begin to appreciate their abundance; it has been estimated that approximately half of all sequenced bacterial genomes contain intact prophages, and even more contain prophage elements (3). Interestingly, the abundance of temperate phages residing in the commensal gut microbiome of mice appears to be even higher (4), indicating that temperate phages may play a role in bacterial community dynamics during colonization. Indeed, many recent studies and reviews have highlighted the importance of phages in the microbiome community (5–8).

One of the ways in which temperate phages influence the biology of their hosts is through lysogenic conversion. During lysogenic conversion, accessory genes encoded on the prophage are expressed in the host cell during lysogeny. These accessory genes influence the biology of the host cell without affecting the phage life cycle. One form of lysogenic conversion is seroconversion in which bacteriophages encode proteins that alter the structure of the host lipopolysaccharide (LPS) O-antigen. The most well-known seroconverting phages are those that infect *Shigella flexneri*; lysogeny with these phages results in modification of the O-antigen through either glucosylation or O-acetylation, leading to a change in bacterial serotype (9). This can have different benefits for the bacterial host, including antigenic variation and immune evasion, since the mammalian innate immune system mounts a serotype-specific antibody response (9). Beyond immunogenicity, LPS is an essential component of the outer membrane that is important for membrane stability and barrier function (10).

Here, we describe the isolation and characterization of novel bacteriophage Kapi1, capable of O-antigen modification. Kapi1 was isolated from a wild commensal strain of *E. coli*, and the phage genome was sequenced and compared to other characterized phages. We also report the identification of the O-antigen as the receptor for Kapi1 and show that this phage displays an unstable temperate lifestyle. Our characterization of Kapi1 suggests that it has a significant impact on the fitness of *E. coli* in the GI environment and that it should serve as an excellent model system to explore the impact of temperate bacteriophage on *E. coli* colonization of the mammalian GI tract.

RESULTS AND DISCUSSION

Kapi1 is a novel *Podoviridae* with a narrow host range. Recently, Lasaro et al. (11) showed that the Cpx, Arc, and Rcs two-component systems found in *Escherichia coli* were required for colonization of the murine GI tract by a strain of commensal *E. coli*, MP1. We began performing competitions between Cpx, Arc, and Rcs mutants and wild-type (WT) MP1 *in vitro* to further explore the molecular mechanisms behind the observed colonization phenotypes. MP1, MP7, and MP13 are identical strains except for the presence of fluorescent plasmids pML8 and pAS07 integrated into the chromosomes of MP7 and MP13, respectively, at the λ attachment site (11). Because MP7 and MP13 are marked with *mcherry* and *gfpmut3.1*, these strains are easily distinguishable during coculture competition experiments. Unexpectedly, when coculturing MP13 *rcsB* mutants with MP7, we found that the *rcsB* mutants strongly outcompeted the wild type (WT) (data not shown). Because Lasaro et al. (11) showed that mutation of *rcsB* decreased competitiveness in a mouse colonization model, we wondered if this reflected a differential ability of the Rcs mutant to compete *in vitro* versus *in vivo*, and we set out to investigate this. Because of the strong competitive advantage, we hypothesized that the *rcsB* mutant could perhaps be directly killing the WT in some way. To test if there was a bactericidal factor secreted by the *rcsB* mutant, we isolated the supernatant from cultures of MP13 *rcsB* mutants and spotted it onto lawns of MP7. Unexpectedly, the supernatant cleared the MP7 lawn, and serial dilutions of the supernatant showed spotty clearing, reminiscent of phage plaques. We then screened our entire strain collection of all strains derived from MP1, MP7, and MP13 for their abilities

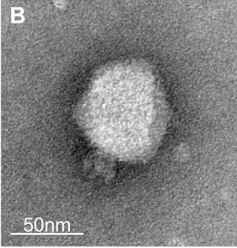
A	Prophage Region	Most Common Phage	Accession	B
	Intact_1	Enterobacteria phage Sf101	NC_027398	
	Questionable_1	Enterobacteria phage DE3	NC_042057	
	Questionable_2	Stx2-converting phage Stx2a-F451	NC_049924	
	Incomplete_1	Bacteriophage APSE-2	NC_011551	
	Incomplete_2	Escherichia phage 500456-1	NC_049342	
	Incomplete_3	Bacillus phage G	NC_023719	

FIG 1 PHASTER analysis of MP1 and transmission electron microscopy image of Kapi1. (A) The genome of MP1 (GenBank accession no. [JEM101000000](https://www.ncbi.nlm.nih.gov/nuccore/JEM101000000)) (11) was analyzed for putative prophage regions using PHASTER (12, 13). Prophage regions identified by PHASTER are shown, including the most common phage from the NCBI viral database, and their corresponding accession numbers. Intact, questionable, and incomplete scores were assigned by PHASTER. (B) Kapi1 phage lysate was stained with 4% uranyl acetate on a copper grid and viewed by transmission electron microscopy at $\times 140,000$ magnification.

to produce plaques on each other. A clear trend emerged; the supernatants of MP1 and MP13 background strains could produce plaques on lawns of MP7, but supernatant derived from MP7 background strains could not produce plaques on either MP1 or MP13. Thus, we began identification and characterization of the phage found in MP1 and MP13.

Because our cultures of MP1 and MP13 containing phages did not appear to have a pronounced growth defect in comparison to MP7, we hypothesized that the phage in these cultures may be temperate, as a lytic phage would be more likely to lyse the cultures, resulting in a visible reduction in cell density and poor growth. Analysis of the previously published genome sequence for MP1 (11) using the prophage identification tool PHASTER (12, 13) revealed six putative prophages integrated into the chromosome of MP1 (Fig. 1A). Of these, only one prophage was scored as intact by PHASTER (12, 13) (Fig. 1A); we hypothesized that this prophage was the most likely candidate for the phage plaques we had observed because of the completeness of the prophage sequence. To confirm this, we performed PCR on colonies of MP1, MP7, and MP13, as well as on phage lysates prepared from MP1 and MP13 with three primer pairs targeting the coat, portal, and tail proteins within the Intact_1 prophage region identified by PHASTER. Bands were consistently observed for MP1 and MP13 colonies and phage lysates and were consistently absent for MP7 colonies for all primer pairs (data not shown). This indicates that the phage present in MP1 and MP13 cultures likely corresponds to the Intact_1 prophage region identified by PHASTER in the MP1 genome. Despite several attempts to induce phage from MP7 using DNA-damaging agents, phage could never be isolated from MP7. Since Lasaro et al. (11) previously showed that MP7 and MP13 had equal competitive indices *in vivo*, we decided to investigate this further. Upon testing the original stock of MP7 isolated by Lasaro et al. (11), we found that this strain does, in fact, contain the Intact_1 prophage region (data not shown) and that only our stock of MP7 lacks the Intact_1 prophage region. These findings are important, as they demonstrate that any competitive advantage that would have been provided by carrying the Intact_1 prophage did not play a role in the findings of Lasaro et al. (11) since both MP7 and MP13 contain the prophage. We therefore renamed our stock of MP7, which lacks the Intact_1 prophage region to KP7, in order to avoid confusion with the original MP7 stock, which does contain the Intact_1 prophage region.

Transmission electron microscopy (TEM) (Fig. 1B) of phage lysates collected from MP1 and MP13 revealed phage particles with a mean capsid diameter of 70.10 ± 2.92 nm and tail length of 15.37 ± 1.45 nm, placing this phage in the family *Podoviridae* and order *Caudovirale*. We screened 11 strains of *E. coli* (TOP10, MG1655, TJ-LM, TJ-WM, TJ-LR, MC4100, W3110, BW25113, J96, E2348/69, and Nissile 1917) and *Citrobacter rodentium* DBS100 for susceptibility to the phage (Table S1 in the supplemental material). TOP10, MG1655, MC4100, W3110, and BW25113 are *E. coli* K-12 derivatives (14), whereas TJ-LM, TJ-WM, TJ-LR, J96, E2348/69, and Nissile 1917 are natural *E. coli* isolates (15–18). All strains were completely resistant to infection; from our strain collection, KP7 is the only strain that this

phage can infect. PHASTER analysis of each of the strains tested shows no predicted prophage regions similar to the Intact_1 prophage region identified in MP1; it is therefore unlikely that they are protected from infection via superinfection immunity, but we cannot rule this out entirely, as all strains tested are lysogenized by several prophages (data not shown). This preliminary analysis suggests that the newly isolated phage has a relatively narrow host range, a trend which has been observed in other temperate phages isolated from the gut (19). This phage forms diffuse plaques on KP7 with an average plaque diameter of 2.0 ± 0.22 mm after overnight incubation at 37°C. Although the morphology of phage particles on TEM and plaques on soft-agar overlays were consistent, to confirm that the Intact_1 prophage region is the only prophage in MP1 capable of active excision and lytic replication, we performed PCR on DNase-treated phage lysates using primers corresponding to each putative prophage region identified by PHASTER and a *nuoA* primer pair to control for genomic DNA contamination. No bands were observed in KP7 lysates, and only the band corresponding to Intact_1 prophage was observed in the MP13 lysate (Fig. S1).

Kapi1 lacks sequence homology with other *Podoviridae* and has a modular lambdoid genome. Although the whole-genome sequence for MP1 has already been published (11), to be thorough and ensure that the isolated phage was truly a prophage and not introduced by contamination from our laboratory, whole-genome sequencing was performed on our stocks of MP1, KP7, and MP13. We also aimed to find the integration site and characterize the genome of the isolated phage. As anticipated, the 39 kb Intact_1 prophage region was present in the genomes of MP1 and MP13 and absent from the genome of KP7. Unfortunately, the phage genome was assembled into its own linear contig, not showing where it may be integrated into the host chromosome. This was observed in both the original MP1 sequence (11) and in our resequencing attempt; it is likely that the phage genome was in its circular form (i.e., excised from the host chromosome) since we extracted DNA from late-stationary-phase cultures. Upon closer analysis of the original MP1 sequence (11), it appears that the ends of contig, GenBank accession no. [NZ_JEM101000030](#), corresponding to the Intact_1 prophage region, are actually terminal repeats, indicating that the sequence is circular. To confirm this circularity, primers were designed pointing outward from each end of the phage contig (prophage_left and prophage_right primers; Table S2), and PCR and Sanger sequencing were performed on DNA extracted from phage lysates. The sequence of the PCR product obtained was consistent with the conclusion that the phage exists in a circular form at some point during its life cycle and confirmed complete sequencing of the entire phage genome.

When the phage genome was analyzed using BLASTn (20) with the viral filter (TaxID 10239), the top hit was *Enterobacteria* phage Sf101 (GenBank accession no. [NC_027398.1](#)) with 96.47% identity but only 33% query cover, indicating that this phage represents a novel viral species with less than 95% nucleotide sequence similarity to any other characterized phage (21). We thus named this novel phage vB_EcoP_Kapi1 (Kapi1; NCBI TaxID 2746235). When the viral filter is removed, the top hit still only shows 96.92% identity and 44% query cover to Kapi1 (*E. coli* genome assembly FHI87; scaffold-10_contig-14.0_1_42036; GenBank accession no. [LM996987.1](#)). Visualization of the alignments between Kapi1 and Sf101 (Fig. 2) showed that an ~10-kb region of Kapi1 corresponding to the virion morphogenesis module is the most conserved region. Further, Kapi1 may represent a novel genus of the family *Podoviridae* since it shares less than 50% nucleotide sequence similarity to any other characterized *Podoviridae* genus (21). Comparing the genome sequence of Kapi1 against the type species for each *Podoviridae* genus in the ICTV 2019.v1 Master Species List (<https://talk.ictvonline.org/files/master-species-lists/>), the top hit, *Enterobacteria* phage P22 (GenBank accession no. [NC_002371.2](#)), belonging to the genus *Lederbergvirus*, shares only 83.62% identity and 20% query coverage with Kapi1. The taxonomy of Kapi1 was further explored using vContact2 (22); this analysis showed that Kapi1 belongs to the same viral cluster as phages P22 (23) and Sf101 (24) (Fig. S2).

The genome of Kapi1 (GenBank accession no. [MT813197](#)) is 39,436 bp in length and represents 0.83% of the genome of MP1. The GC content of Kapi1 is 47.1%, slightly

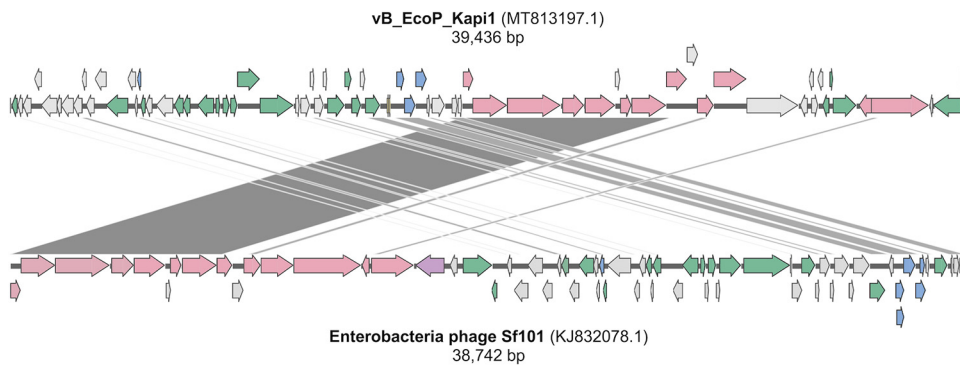


FIG 2 Genome of Kapi1 and alignment with the most closely related phage, Sf101. (Top) Layout of the Kapi1 genome, with ORFs color-coded as follows: lysis module in blue, structural/morphogenesis in pink, DNA replication/repair/regulation in green, tRNAs in yellow, and hypothetical proteins and proteins of unknown function in gray. (Bottom) Alignment of the Kapi1 genome against the genome of phage Sf101 is visualized with Kablammo (86); darker lines represent higher sequence homology between the two phages. Sf101 seroconversion protein (*gp16* O-acyltransferase B) is indicated in purple.

lower than the 50.6% of the host genome. Kapi1 has a modular genome structure typical of many lambdoid phages (Fig. 2) (25). Beginning from *xis*, the first region of the Kapi1 genome is rich in hypothetical proteins and proteins with unknown function. The next segment of the genome is characterized by the DNA replication/repair/regulation module; this region has a lambda-like organization, with CIII, N, CI, *cro*, CII, O, P, and Q. This module is followed by two tRNAs immediately preceding the lysis module (*holin*, *lysins*, and *Rz*). The next module is responsible for virion morphogenesis, encoding proteins responsible for the head assembly (*terminases*, *scaffold*, *portal*, and *coat*), followed by tail assembly (*DNA stabilization protein*, *tail needle knob*, and *DNA transfer and ejection proteins*). The final module is required for integration, including *xis*, *int*, and *attP*. For a detailed view of annotation and functional assignments for all protein-coding sequences (CDSs) in Kapi1, see Table S3.

Kapi1 integrates into the 3' end of host tRNA *argW*. To begin our search for the integration site of Kapi1, we used BLASTn (20) to look for prophages similar to Kapi1 in the NCBI nucleotide database. We then analyzed the host chromosome surrounding these Kapi1-like prophages to find any similarities with the MP1 chromosome. We identified two contigs in MP1 whose ends shared significant similarity to the regions surrounding Kapi1-like prophages found in the NCBI database. The end of the first contig encodes the *dsdAXC* genes, while the end of the second contig encodes *yfdC*, *mIaA*, and *fadLIJ* genes. Primer pairs were designed to amplify the putative prophage-chromosome junctions (prophage and chromosome_left; prophage and chromosome_right primers) (Table S2); PCR products were then sequenced and aligned with the original sequences to determine the integration site of Kapi1 and its orientation in the host chromosome. Kapi1 integrates into the chromosome between genes *yfdC* and *dsdC*, with the phage *int* gene closest to the chromosomal *yfdC* locus and the phage *xis* gene on the opposite end of the prophage closest to the chromosomal *dsdC* gene (Fig. 3A). Notably, the way in which the original MP1 sequence (11) was assembled actually captures the chromosome-prophage left_junction (Fig. 3A) since the end of contig, GenBank accession no. [NZ_JEM101000016](https://www.ncbi.nlm.nih.gov/nuclot/NZ_JEM101000016), contains Kapi1 *xis* (annotated as *TorI* in the original sequence) directly downstream of *dsdC*. *yfdC* is a predicted inner membrane protein belonging to the formate-nitrate transporter family and may be involved in resistance to surfactants (26); *dsdC* is a transcriptional regulator involved in D-serine detoxification (27). This region of the genome is hypervariable among different *E. coli* pathotypes, and a variety of prophage- and phage-like genes are often found at this locus (28).

With the integration site for Kapi1 identified, we then looked back at our whole-genome sequencing data for KP7, the strain lacking the Kapi1 prophage. In this strain, the integration locus was correctly assembled; the two contigs that we confirmed to

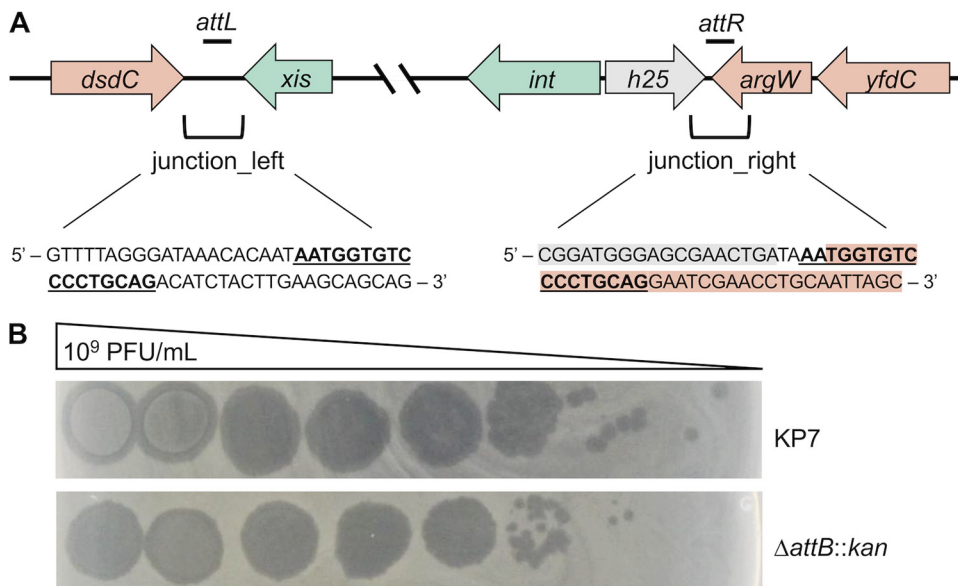


FIG 3 Integration site of Kapi1. (A) The structure of Kapi1 integrated into the host chromosome; host ORFs are indicated in orange, and phage ORFs are indicated in green and gray in between the *attL* and *attR* sites. Nucleotide sequences are provided for both the left and right host-prophage chromosome junctions, including 20 bp upstream and downstream of the bolded and underlined *att* sites. Gray shading on the junction_right sequence indicates the location of the Kapi1 *hyp25* gene, and orange shading indicates the host *argW* gene. (B) Kapi1 phage lysate was serially diluted and spotted onto soft-agar overlays of either WT KP7 or KP7 $\Delta attB::kan$.

surround the integrated Kapi1 prophage in MP1 were assembled into one complete contig in KP7. We noticed a tRNA-Arg in between *dsdC* and *yfdC* that was not annotated on the contigs surrounding the Kapi1 prophage in MP1. Since tRNAs are common integration sites for phage (29), this site was further investigated. When we investigated the chromosomes of MP1 and MP13 with the Kapi1 prophage integrated as described above, we noticed a 17-bp duplication on either end of the integrated prophage; this sequence (5'-AATGGTGTCCCCTGCAG-3') is found at the 3' end of the tRNA-Arg and is the putative Kapi1 *att* site (Fig. 3A). To be clear, this tRNA-Arg is intact whether or not Kapi1 is integrated into the chromosome since the 3' end is maintained by the Kapi1 putative *attP* when it integrates into the chromosome. The *attB* site was not picked up by the auto-annotation programs in MP1 and MP13 since, during sequencing, the two contigs surrounding Kapi1 were not assembled into the correct scaffold, as they were in KP7.

Interestingly, the Kapi1 putative *attP* is identical to prophages Sf6 (30), HK620 (25), and KplE1 (31) except for the 5' A, which is excluded from the Sf6, HK620, and KplE1 *attP* sites. Like these phages, the Kapi1 *attP* lies between the *int* and *xis* genes, so upon integration into the host chromosome, the *int* and *xis* genes are located on either end of the prophage (Fig. 3A). We generated a KP7 $\Delta attB::kan$ mutant resulting in a precise deletion of the 17-bp putative *attB* and replacement with a kanamycin (Kan) resistance cassette; Kapi1 retains the ability to infect and replicate within this host (Fig. 3B). We next determined the efficiency of lysogeny by Kapi1 of WT KP7 compared to KP7 $\Delta attB::kan$ by infecting each strain with Kapi1 at a multiplicity of infection of 10 and plating out survivor colonies. Using primers that span the prophage_left junction, we consistently observed bands for WT KP7 (19/20 colonies screened) but never observed bands for KP7 $\Delta attB::kan$ (0/24 colonies screened). When these colonies were grown overnight and their supernatant was spotted onto a lawn of naive KP7, all KP7 cultures produced zones of clearing on KP7, and only 3/24 $\Delta attB::kan$ colonies produced zones of clearing. Since these $\Delta attB::kan$ survivor colonies did not appear to have any growth defect in comparison with WT KP7 survivor colonies, it seems unlikely that they were

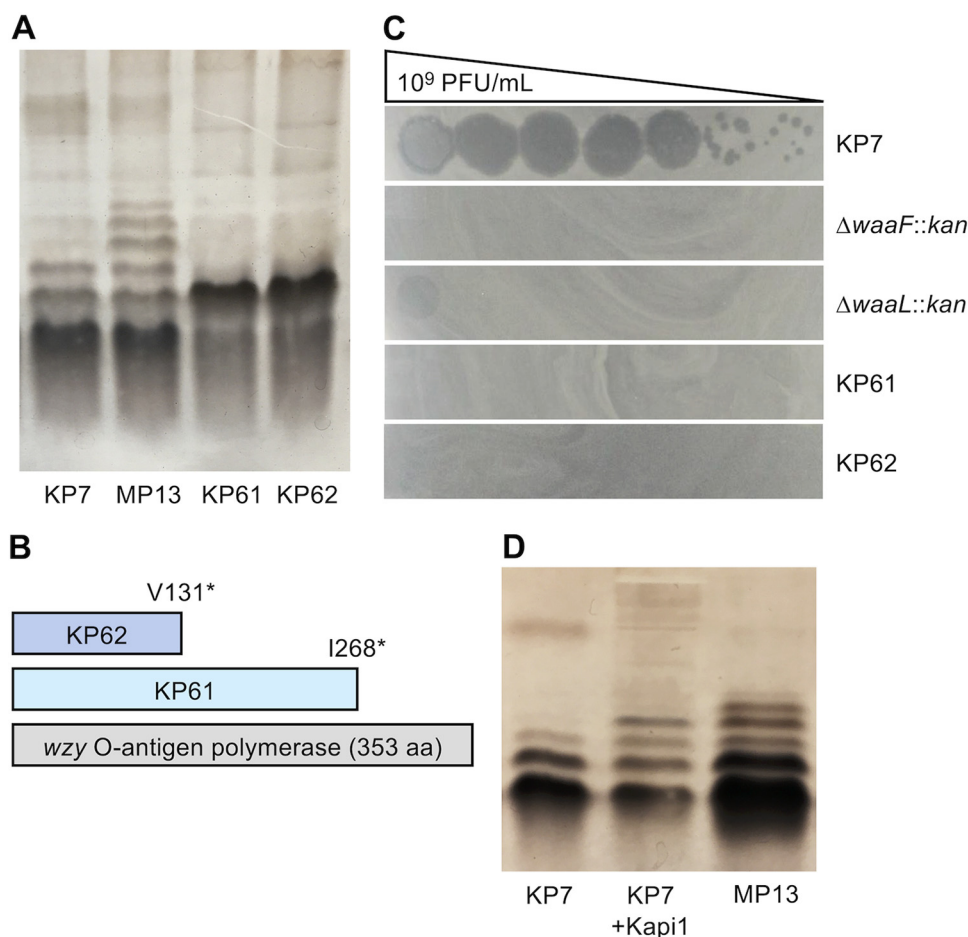


FIG 4 Kapi1 uses the O-antigen as a receptor and modifies its structure. (A) LPS extracted by proteinase K digestion was run on SDS-PAGE and silver stained; spontaneous Kapi1-resistant mutants in lanes 3 and 4 correspond to KP61 and KP62, respectively. (B) Schematic representing the truncated *wzy* polymerase from KP61 and KP62 compared with the full-length WT protein. (C) Kapi1 phage lysate was serially diluted and spotted onto soft-agar overlays with a variety of mutants in the KP7 background. (D) Phenol-extracted LPS was run on SDS-PAGE and silver stained; in lane 2, KP7 LPS was treated with Kapi1 phage prior to running on SDS-PAGE.

lytically infected with Kapi1, and we propose that, rather, they were lysogenized with Kapi1 via integration at an alternative *att* site elsewhere in the genome.

The Kapi1 receptor is LPS O-antigen and is modified by Kapi1 both during initial binding and later during lysogeny. Many phages use LPS as a receptor for host cell infection, particularly *Podoviridae* (32), including phages HK620 (33) and P22 (23), among others. Based on this knowledge, we hypothesized that Kapi1 may use LPS as its receptor. We isolated spontaneous mutants resistant to Kapi1 by picking survivor colonies from lawns of KP7 overlaid with Kapi1. Since Kapi1 is temperate, survivor colonies were screened for lysogeny by colony PCR with primers spanning the prophage-chromosome junction and by growing survivor colonies overnight and spotting their supernatant onto KP7. Two Kapi1-resistant survivor colonies were verified to not be lysogenized by Kapi1 and were chosen for further analysis (KP61, KP62). LPS profiling by SDS-PAGE and silver staining showed that the Kapi1-resistant mutants have severely truncated LPS compared to the WT (Fig. 4A). The genomes of KP61 and KP62 were sequenced, and variant calling was performed using WT KP7 as a reference. Both Kapi1-resistant strains contained only one mutation relative to WT, a 1-bp deletion in the *wzy* polymerase causing a frameshift resulting in a truncation (Fig. 4B; Fig. S3). Mutations in *wzy* result in synthesis of a complete core LPS, but only 1 O-unit is displayed on the cell surface (34), instead of the usual long-chain O-antigens, consistent

with what was observed on silver staining. These results indicate that Kapi1 likely binds the KP7 O-antigen as its primary receptor; however, it appears that 1 O-unit is insufficient for recognition, as *wzy* mutants are completely resistant to infection (Fig. 4C).

To confirm that O-antigen is the receptor for Kapi1, we proceeded to create two LPS mutants, KP7 $\Delta waaL::kan$, which has a complete core but no O-antigen (35), and KP7 $\Delta waaF::kan$, which has a severely truncated core structure consisting of lipid A, Kdo₂, and heptose (36). Surprisingly, KP7 $\Delta waaL::kan$ is able to be infected by Kapi1, but at an extremely low efficiency (faint clearing in undiluted spot; Fig. 4C), whereas KP7 $\Delta waaF::kan$ is completely resistant to infection by Kapi1 (Fig. 4C). This indicates that in the absence of O-antigen, Kapi1 may be able to recognize a portion of the outer core structure that is intact in $\Delta waaL::kan$ but absent in $\Delta waaF::kan$ as a secondary receptor; in KP61 and KP62, the single O-unit may obscure this secondary receptor to prevent Kapi1 recognition/binding. Interestingly, *E. coli* W3110 *waaF* mutants have been shown to not produce flagella (37), so this presents another putative secondary receptor for Kapi1. However, no individual plaques can be observed when Kapi1 is spotted on KP7 $\Delta waaL::kan$ (Fig. 4C), so it is also possible that the spot is the result of bactericidal activity and not a productive phage infection (38). In light of the identification of the O-antigen as the receptor for Kapi1, our previous host range results make sense; many of the strains we tested lack O-antigen (K-12 derivatives MC4100, MG1655, BW25113, and W3110), and those that do produce O-antigen (natural isolates E2348/69, J96, DBS100, TJ-LM, TJ-WM, TJ-LR, and Nissile 1917) do not appear to have the same O-antigen structure as KP7 on silver-stained SDS-PAGE (data not shown). Although the data presented here are not an extensive screen of all possible serotypes of *E. coli*, it is possible that Kapi1 is specific to one or a few serotypes; identification of the precise region of O-antigen that Kapi1 recognizes as its receptor will help to clarify these results.

While performing LPS profiling in the previous experiments, we noticed that the LPS profiles of MP1 and MP13 differed from the LPS profile of KP7 (Fig. 4A). We hypothesized that the change in LPS structure was due to lysogenic conversion by Kapi1. Several of the bacteriophages most similar to Kapi1 have been shown to cause seroconversion in their respective hosts. Phages Sf101 and Sf6 both encode O-acetyl transferases to cause seroconversion in their host, *S. flexneri* (24, 39), and phage P22 encodes an O-antigen glucosylation cassette (*gtrABC*) to cause seroconversion in its host *Salmonella enterica* serovar Typhimurium (40). We began by searching for CDSs in the genome of Kapi1 with homology to known seroconversion proteins. Although none of the CDSs in Kapi1 were annotated as possible O-antigen-modifying/seroconverting proteins, closer examination revealed limited regions of homology to known seroconversion proteins in a few CDSs. Kapi1 hypothetical protein 5 (*hyp5*) has limited homology with viral acetyltransferases (90% query coverage and 54.36% amino acid identity to *Mycobacterium* phage proph68-1 acetyltransferase; GenBank accession no. [QSM02012.1](#)) and acyltransferases (68% query coverage and 57.14% amino acid identity to uncultured Mediterranean phage uvMED putative acyltransferase; GenPept accession no. [BAR19615.1](#)). Using a targeted search approach, we looked for homology to a set of known viral seroconversion proteins in the Kapi1 genome and found that Kapi1 hypothetical protein 19 (*hyp19*) has a small region of limited homology with an inhibitor of alpha polymerase (*iap*) encoded by *Salmonella* phage epsilon15 (2% query coverage with 47.62% percent amino acid identity; GenBank accession no. [NP_848230](#)). Many of the phages infecting *S. flexneri* that are closely related to Kapi1 encode seroconversion genes that are located near the *int-att-xis* region of the genome (9), so we included two additional CDSs as putative seroconversion proteins due to their location in the genome and lack of homology to any known proteins in the NCBI viral BLASTp database, Kapi1 hypothetical protein 24 (*hyp24*) encoded between the tail spike protein and integrase and hypothetical protein 25 (*hyp25*) encoded between the integrase and *attP* site.

We cloned each of these four putative seroconversion proteins into the pTrc99a overexpression vector (41) and introduced them into KP7 and then compared the LPS

profiles of each overexpression strain, the vector control, and WT KP7 and MP13. Unfortunately, none of the strains overexpressing the four putative seroconversion proteins from Kapi1 had altered LPS profiles (data not shown). Although none of these proteins were found to be individually responsible for seroconversion, we could not eliminate the possibility that they could be working with other phage-encoded proteins to produce the altered LPS phenotype, as there are numerous examples of seroconverting phages that encode entire gene cassettes responsible for seroconversion, including *Pseudomonas aeruginosa* phage D3 (42) and *Salmonella* phage P22 (40). We thus individually deleted *hyp5*, *hyp24*, and *hyp25* from Kapi1 lysogens and examined LPS profiles via silver-stained SDS-PAGE; once again, none of these genes were found to be responsible for Kapi1-mediated O-antigen modification, as the LPS profiles of each mutant were identical to the WT lysogen (data not shown). Notably, we were unable to delete *hyp19*. Both TOP10 (Invitrogen) cells carrying pUC18 (43) with the Δ *hyp19* construct and our conjugative donor strain MFDpir (44) carrying the suicide vector pRE112 (45) with the Δ *hyp19* construct had quite severe growth defects. We hypothesize that this may be due to one of the hypothetical proteins flanking *hyp19* that is present on the deletion construct exerting some type of toxicity in these strain backgrounds, which are not lysogenic for Kapi1. Additionally, when screening Kapi1 lysogens for double-crossover events (in which the pRE112 vector backbone is excised from the chromosome via homologous recombination, leaving either the WT copy of *hyp19* or Δ *hyp19* behind), we noted an unusually high rate of Kapi1 excision. Only 9/2,000 colonies screened retained the Kapi1 prophage (0.45%), while under normal conditions, approximately 90% of the population retains the Kapi1 prophage after 24 h of growth in LB (data not shown).

Although we were unsuccessful in identifying the gene responsible for Kapi1-mediated O-antigen modification, it is interesting that the genetic basis for this O-antigen modification by Kapi1 appears to not be well conserved, as no strong hits to known O-antigen-modifying proteins could be identified. It will be valuable to determine the molecular mechanisms behind Kapi1 phage-mediated O-antigen modification and whether these mechanisms are indeed novel. Since we identified the LPS O-antigen as the receptor for Kapi1, and Kapi1 lysogens are protected from superinfection by Kapi1, there is a distinct possibility that Kapi1-mediated O-antigen modification is a mechanism for the observed superinfection immunity. If the modified LPS displayed on the cell surface of Kapi1 lysogens is unable to be bound by Kapi1 phage, this could prevent superinfection by Kapi1 or similar O-antigen binding phages. Besides superinfection immunity, modification of the LPS O-antigen could alter the immunogenicity of Kapi1 lysogens if, for example, this modification leads to a change in serotype. However, what the relevance of this would be for a nonpathogenic strain of *E. coli* such as MP1 is unclear. Finally, modification of the O-antigen structure could alter the barrier function of LPS, resulting in, for example, altered resistance to antibiotics or altered membrane rigidity (10).

Phages that use the O-antigen as a receptor also commonly modify the O-antigen using the tail spike protein (*tsp*) to facilitate movement to the bacterial outer membrane, where irreversible binding and particle opening can occur (46). To determine if O-antigen degradation via *tsp* was instead responsible for the altered LPS structure between Kapi1 lysogens and nonlysogens observed on SDS-PAGE (Fig. 4A), we mixed Kapi1 with purified KP7 LPS and ran these samples alongside purified LPS from KP7 and MP13 (not mixed with Kapi1 phage). It appears that treatment of purified KP7 LPS with Kapi1 results in an altered LPS structure (suggesting degradation of O-antigen by Kapi1), but this structure is different from that of either the WT or lysogenic backgrounds (Fig. 4D). Therefore, Kapi1 is responsible for alteration of the LPS structure, both upon binding O-antigen prior to infection and later via lysogenic conversion. Kapi1 *tsp* has considerable sequence conservation in the head-binding domain (most similar to phages HK620 and Sf101) but no sequence similarity to any other viral proteins in the NCBI database along the length of the protein. Therefore, it is difficult to

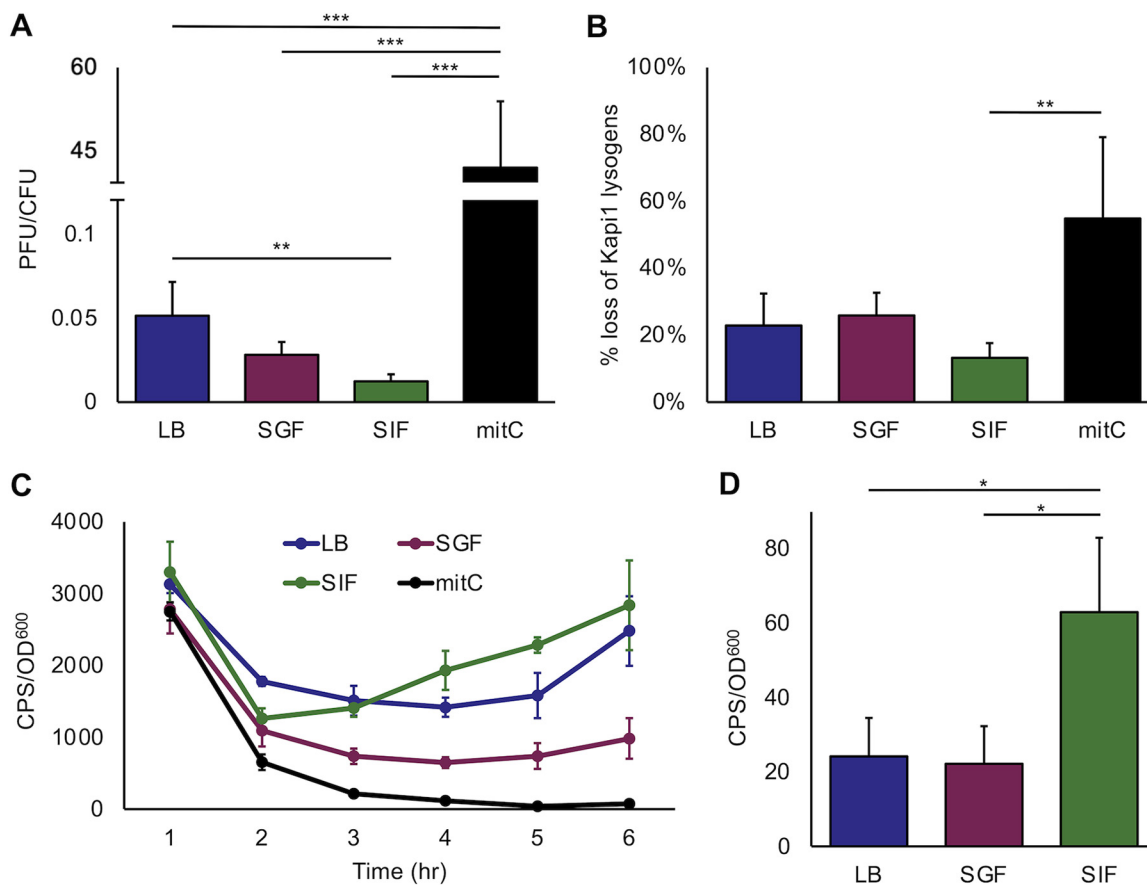


FIG 5 Stability of Kapi1 lysogens grown in different media. (A) Cultures of MP13 (Kapi1 lysogen) were grown in LB, 50% LB with 50% simulated gastric fluid (SGF) (50), 50% LB with 50% simulated intestinal fluid (SIF) (50), or LB supplemented with 0.5 ng/ μ l mitomycin C for 24 h. After 24 h, the number of cells was enumerated by spotting on LB plates, and the number of phages were enumerated by spotting on soft-agar overlays prepared with KP121. PFU/mL was divided by CFU/mL to obtain PFU/CFU; the values represent the average of three biological replicates, and error bars represent the standard deviation. One outlier value was excluded for the mitomycin C treatment. A one-way ANOVA was performed with a Tukey's *post hoc* test on log-transformed data. (B) MP13 was grown in the same media as above for 24 h and then subcultured into fresh media and grown for another 24 h. After 48 h total incubation, cells were plated onto LB agar and then replica plated onto a second LB agar plate spread with KP7 to screen for Kapi1 lysogens (Fig. S5 in the supplemental material). The number of nonlysogenic colonies was divided by the total number of colonies to obtain percent loss of Kapi1; values represent the average of three biological replicates, and error bars represent the standard deviation. A one-way ANOVA was performed with a Tukey *post hoc* test on arcsine-transformed data. (C) Luminescent reporter assay. The activity of Kapi1 *Cl-lux* was monitored in Kapi1 lysogens grown in the same media as above. The average luminescence (counts per second [CPS]) normalized to bacterial optical density (OD_{600}) is reported for three biological replicates, and error bars represent the standard deviation. (D) *Cl-lux* activity after 24 h of growth. The average normalized luminescence is reported for three biological replicates, and error bars represent the standard deviation. A one-way ANOVA was performed with a Tukey *post hoc* test.

predict what type of enzymatic activity the Kapi1 *tsp* may have, and further work is needed to characterize the molecular mechanisms of Kapi1-mediated O-antigen modification through *tsp*.

Kapi1 is an unstable temperate phage and shows an altered lifestyle in simulated intestinal conditions. To investigate the lifestyle of Kapi1, we measured the titer of Kapi1 along with host cell counts in cultures of lysogens. After only 24 h of growth, $\sim 1 \times 10^8$ PFU/mL can be isolated from standard laboratory cultures of lysogens (data not shown). The ratio of phages per cell (PFU/CFU) in cultures of lysogens is only 0.050 ± 0.020 after 24 h of growth and rises to 41.66 ± 11.79 PFU/CFU when identical cultures are grown with subinhibitory concentrations of mitomycin C (Fig. 5A). This suggests that Kapi1 can be induced by mitomycin C through the traditional SOS pathway in response to DNA-damaging agents, although there appears to be a basal level of spontaneous induction even in the absence of mitomycin C. The classical mechanism of SOS-mediated prophage induction as set by the widely studied phage λ is dependent on an activated form of *recA*, which mediates autocleavage of the λ repressor, *cl* (47). *recA* is activated by the presence

of single-stranded DNA and mediates the autocleavage of *lexA* (48), which is the major repressor protein of the SOS response. Upon cleavage of the *lexA* repressor, SOS-regulated genes are then derepressed, resulting in a full SOS response (for a review of the SOS response, see reference 49). To determine if Kapi1 lytic replication is *recA* dependent, we repeated the above-described assay in a $\Delta recA::kan$ lysogen background and did not observe plaque formation in either the presence or absence of mitomycin C (data not shown), indicating that both spontaneous and DNA damage response induction of Kapi1 occur in a *recA*-dependent manner. Whether the Kapi1 CI repressor protein is directly cleaved by activated *recA*, or if this lytic defect is due to the downstream effect of SOS-regulated genes remaining repressed by *lexA*, is yet to be determined.

Since MP1 was recently isolated from the feces of a healthy mouse (11) and is more host adapted than our standard laboratory strains of *E. coli* such as MG1655 or MC4100, we wondered if Kapi1 might be important to the biology of commensal *E. coli* in the GI tract. To investigate the biology of Kapi1 under more physiologically relevant conditions, we repeated the same experiments following the numbers of phage and host cells in media composed of 50% LB and 50% simulated intestinal fluid (SIF) as well as 50% LB and 50% simulated gastric fluid (SGF) (50). We found lower ratios of Kapi1 PFU to host CFU in SIF than LB (Fig. 5A), although the strains grow to nearly identical cell densities. Importantly, the rate of Kapi1 adsorption to host cells is equal across all tested medium types (Fig. S4A), and Kapi1 phage particles are stable in each medium tested (Fig. S4B); thus, we conclude that the differences in PFU/CFU ratios reflect the approximate induction rates of Kapi1. We next performed prophage stability assays, which showed that upon repeated subculturing of a lysogen, the percentage of the population carrying Kapi1 reduces by approximately 10% upon each successive subculture in LB and that the lysogen population is more stable in media composed of 50% LB and 50% SIF (Fig. 5B). This result supports our previous finding that the original MP7 isolate lost the Kapi1 prophage before arriving at our lab, likely during handling or passaging. Finally, we monitored the expression of Kapi1 CI using a luminescent reporter assay. The regulatory region of the Kapi1 genome is well conserved and is reminiscent of phage λ , which famously uses the CI phage repressor to maintain lysogeny (reviewed in reference 51). We thus cloned the promoter region of Kapi1 CI (−86 to +13) into the luminescent reporter plasmid pNLP10 (52) and monitored light production as an indicator of CI expression and thus maintenance of the lysogenic cycle. Monitoring CI-*lux* activity over time revealed interesting gene expression patterns; we found that when Kapi1 lysogens are grown in SIF, CI-*lux* activity increases after 2 h of growth (Fig. 5C). In contrast, the CI-*lux* expression patterns in LB and SGF do not show this induction and, instead, plateau throughout exponential growth (Fig. 5C). We also included a culture grown with subinhibitory concentrations of mitomycin C and, as expected, noted the lowest CI-*lux* activity under this condition (Fig. 5C). After 24 h of growth, we again measured CI-*lux* activity and observed increased CI-*lux* in SIF compared to both LB and SGF (Fig. 5D), supporting our previous results (Fig. 5A to C). Interestingly, there seems to be an initial adjustment period between 0 and 2 h after mid-log-phase cells are introduced into new media where CI-*lux* activity sharply decreases in all medium types tested (Fig. 5C). We note that even cells grown in LB, briefly pelleted, and then resuspended in LB show this same drop in CI-*lux* activity, indicating that this could be a response to cell pelleting or other experimental factors independent of medium type. Alternatively, this could be a growth phase-dependent phenotype only observed during early exponential phase; however, we did not explore this phenomenon further.

The previous three assays agree; there is a lower level of Kapi1 induction when lysogens are grown in LB supplemented with SIF compared to LB alone or LB supplemented with SGF, and this low level of induction is likely responsible for the increased stability of the lysogen population in media supplemented with SIF. This result is unexpected because LB is considered a nonstressful standard lab media, yet there is a higher proportion of spontaneous phage induction under this condition compared to

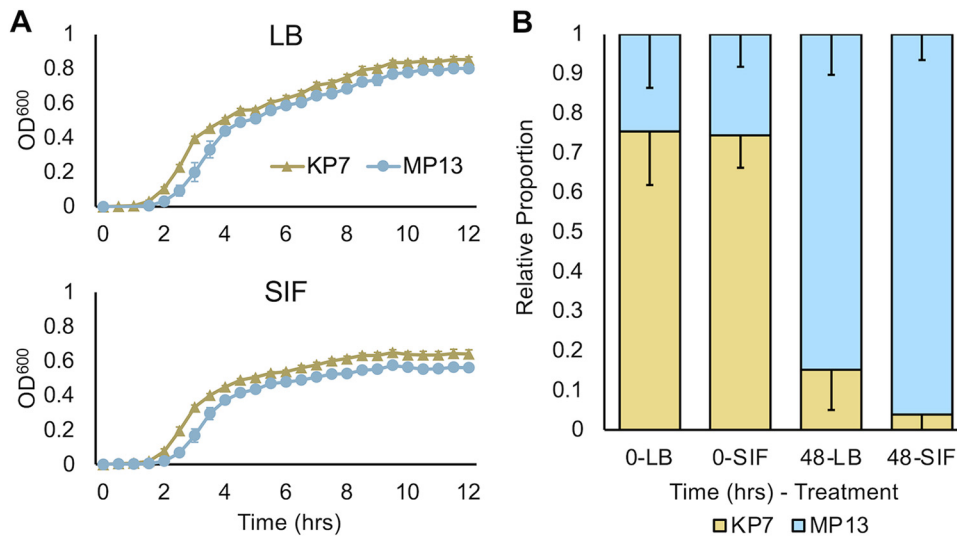


FIG 6 Kapi1 lysogens have a competitive advantage over their nonlysogenic counterparts *in vitro*. (A) Growth curves were performed with KP7 and MP13 grown in either LB or SIF at 37°C. Optical density was measured every 30 min for 12 h; the mean and standard deviation of 3 biological and 2 technical replicates ($n = 6$) are shown. (B) *In vitro* competitive assay. KP7 and MP13 were cocultured in either LB or SIF. Each strain was enumerated every 24 h, after which cocultures were subcultured into fresh media and grown for an additional 24 h. The relative proportion of each strain was calculated by dividing KP7 or MP13 CFU/mL by the total CFU/mL. The average of 3 biological replicates is reported, with the standard deviation as error bars. A *t* test assuming unequal variance was performed on arcsine-transformed data at $t = 48$ h and found no statistical significance between the two treatments ($P > 0.05$).

a less rich and more challenging simulated intestinal medium (Fig. 6A). Additionally, since the PFU/CFU in LB diluted 50% with either distilled water or phosphate-buffered saline (PBS) were nearly identical to full LB (Fig. S4C), it seems likely that the lower rate of induction observed in SIF is not simply due to dilution of the rich LB media and may be specific to intestinal conditions. Since the rate of Kapi1 induction is lower in SIF and more lysogens are retained in the population in SIF (Fig. 5), this could indicate that lysogeny with Kapi1 is selected for in intestinal conditions. This could mean that when integrated as a prophage, Kapi1 may provide some advantage to the cell which may be dispensable under standard lab conditions. Prophages have been shown to provide fitness benefits to their hosts, including resistance to osmotic, oxidative, and acid stresses, as well as influencing biofilm formation (53); many of these stresses would be encountered during colonization of the mammalian GI tract. Notably, there are also examples where prophages are detrimental to their hosts' overall fitness during colonization of the GI tract (54); our observations regarding the stability of Kapi1 lysogens in simulated intestinal conditions warranted further investigation into how (or if) Kapi1 influences the fitness of commensal *E. coli* during colonization of the GI tract.

Kapi1 confers a competitive advantage to its host during competition with a susceptible host. To investigate how carriage of Kapi1 might impact the overall fitness of its host, we performed competitive assays between KP7 and MP13 in either LB or SIF. Importantly, growth curves of each strain grown individually show that MP13 has a slight growth defect compared to KP7 in both LB and SIF (Fig. 6A), which could impact the relative fitness of MP13. We noted a longer lag phase for MP13 in both LB and SIF (30 min longer than KP7) and a reduced terminal optical density for MP13 in both LB (0.051 lower than KP7) and in SIF (0.079 lower than KP7). Both KP7 and MP13 grow to a lower terminal optical density in SIF than LB (Fig. 6A). To perform competition experiments *in vitro*, we cocultured KP7 and MP13 in either LB or SIF, plating cultures onto tetracycline and enumerating the number of red fluorescent (KP7) and green fluorescent (MP13) colonies every 24 h. MP13 strongly outcompetes KP7, and this competitive advantage is further enhanced when cells are cocultured in SIF compared to LB (Fig. 6B). Although the difference in the relative proportion of each strain between LB

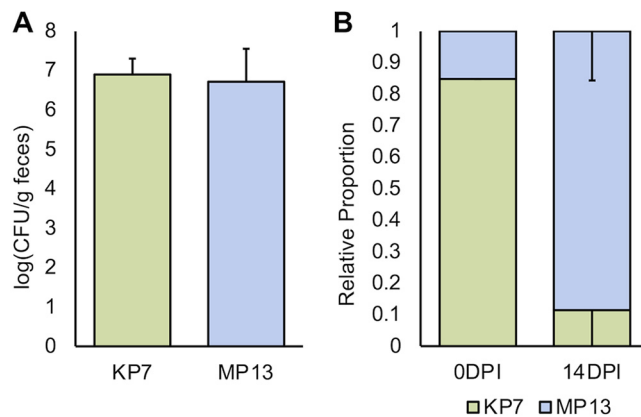


FIG 7 Kapi1 lysogens outcompete their nonlysogenic counterparts during colonization of specific-pathogen-free mice. (A) *In vivo* colonization. Coliform-free mice were gavaged with either KP7 or MP13, and log (CFU/g feces) was enumerated by plating on MacConkey media after 14 days. The average of 4 mice is reported, with standard deviation as error bars. A *t* test assuming unequal variance was performed and found no statistical significance between the two treatments ($P > 0.05$). (B) *In vivo* competitive colonization. Coliform-free mice were gavaged with a mixture of KP7 and MP13, and the relative proportion of each strain was enumerated after 14 days. The average of 10 mice is reported, with standard deviation as error bars.

and SIF after 48 h of coculture is not statistically significant, these results were replicable (data not shown). The increased strength of Kapi1 lysogen competitiveness in SIF supports our previous findings regarding the stability of Kapi1 lysogens in SIF (Fig. 5), suggesting that the interactions between Kapi1 and its host are altered in simulated intestinal conditions compared to standard lab conditions. These findings open the doors to asking meaningful questions about what the precise roles of temperate phages are in the GI tract and how their interactions with their bacterial hosts are altered in this environment compared to a laboratory environment.

To expand on these findings, we next performed competitive assays *in vivo*, utilizing specific-pathogen-free (SPF) mice to study these interactions in the presence of a healthy microbiome. We performed two treatments: mice were treated with either KP7 or MP13 alone (colonization) or a mixture of KP7 and MP13 (competitive colonization). Both KP7 and MP13 stably colonize SPF mice for at least 28 days without significantly impacting mouse body weight (data not shown), but there is no difference in colonization levels between the two strains (Fig. 7A). Interestingly, this result is contradictory to several recent studies exploring the roles of temperate phages in the GI tract, which found that *Lactobacillus reuteri* lysogens have reduced survival during GI transit of conventional mice compared to the identical strain lacking both intact prophages (55, 56). As noted by the authors, the strain of *L. reuteri* used in these studies does not colonize conventional mice (55, 56), so our experiments differ from theirs since MP1 does stably colonize mice (11). Further, it is not surprising that each unique species and each unique phage-host pair may interact with each other and with their surrounding environment in unique ways. These findings highlight the knowledge gap in our current understanding of how temperate phages behave in physiologically relevant conditions.

During competitive colonization of SPF mice, MP13 once again strongly outcompetes KP7 (Fig. 7B), supporting our *in vitro* findings (Fig. 6B). It is interesting to note that despite the observed growth defect of Kapi1 lysogens in Fig. 6A, Kapi1 lysogens are consistently able to outcompete sensitive competitors in a variety of environments (Fig. 6B; Fig. 7B). In contrast to our colonization results (Fig. 7A), our *in vivo* competition results (Fig. 7B) are supported by several recent studies which found that temperate phages provide a competitive advantage to their host when in competition with naive phage-susceptible hosts (54, 56). Notably, both of these competitive studies were performed in germfree mice (54, 56), whereas our competitions were performed in SPF mice in the presence of a healthy microbiome, which we argue is a more

physiologically relevant model of GI colonization. Our findings that Kapi1 lysogens do not have a colonization defect compared to an identical strain lacking Kapi1 and that Kapi1 lysogens are able to outcompete sensitive competitors *in vivo* in the presence of a healthy microbiome are novel findings in this field of research. Importantly, competition is a physiologically relevant condition, as bacteria are never “alone” when colonizing the healthy GI tract; these results warrant further investigation into how temperate bacteriophages modulate community dynamics in these densely colonized environments. Our previous results (Fig. 5) demonstrate that in pure culture, lysogeny (as opposed to lytic induction of Kapi1) is favored in SIF, but whether or not this is maintained during competition, or during GI colonization, is still under investigation. It is tempting to assume that Kapi1 provides a competitive advantage to its host via direct killing of naive competitors, but if lysogeny is, in fact, favored in the intestine as our previous results may suggest, there could be additional factors at play, including lysogenic conversion.

In conclusion, we have isolated and begun the characterization of a novel bacteriophage infecting commensal *E. coli*. The genome of Kapi1 has been sequenced and annotated, and the prophage integration site in the host genome has been identified. Further, we demonstrate that Kapi1 shows unstable lysogeny and that lysogeny appears to be selected for in intestinal conditions. O-antigen is the Kapi1 receptor, and Kapi1 appears to modify the host O-antigen upon initial binding and later in infection through lysogenic conversion, although the molecular mechanisms are yet to be elucidated. Our findings show that Kapi1 lysogeny confers a competitive advantage during colonization of the mouse GI tract, and we propose that MP1 and Kapi1 will serve as a good model system to explore what role(s) temperate phages may play in colonization of the GI tract by commensal strains of *E. coli*.

MATERIALS AND METHODS

Bacterial strains and growth conditions. Strains MP1, MP7, and MP13 were a generous gift from the Goulian lab (11). A complete list of bacterial strains used in this study can be found in Table S1 in the supplemental material. Unless otherwise specified, all strains were grown in LB (10 g/L tryptone, 5 g/L NaCl, and 5 g/L yeast extract) supplemented with the appropriate antibiotics, at 37°C and 225 rpm. When plated, cells were grown on LB 1.5% agar supplemented with the appropriate antibiotics and incubated inverted at 37°C. Antibiotic concentrations used are as follows: 100 $\mu\text{g}/\text{mL}$ ampicillin, 30 or 50 $\mu\text{g}/\text{mL}$ kanamycin, and 15 $\mu\text{g}/\text{mL}$ tetracycline. All chemicals were obtained from MilliporeSigma Canada.

Phage isolation, propagation, host range, and transmission electron microscopy. Phages were isolated from overnight cultures of MP1 or MP13 by pelleting cells, and filter sterilizing the supernatant using a 0.45- μm syringe-driven filter. Individual plaques were isolated and propagated, and phage stocks prepared by previously described methods (57) and slightly modified. Briefly, the above phage-containing supernatant was mixed with susceptible host strain KP7 1:1; then, 3.5 mL soft agar (LB 0.7% agar) was added, and the mixture was poured onto solid LB agar plates and incubated overnight. Individual plaques were picked with a sterile Pasteur pipette and gently resuspended in 500 μL modified suspension media (SM) (50 mM Tris-HCl [pH 7.4], 100 mM NaCl, and 10 mM MgSO_4). This suspension was then amplified using the soft-agar overlay technique as above. Plates with near-confluent lysis were used to prepare high-titer stocks by collecting the soft agar layer as follows: SM was poured onto the surface of the plate, and soft agar was gently scraped into a 50-mL Falcon tube using a sterile scoopula, rocked at room temperature for 1 h, and centrifuged to pellet the soft agar. The supernatant was filter sterilized using a 0.22- μm syringe-driven filter and stored at 4°C. Plaque diameter was measured from 10 plaques, using Fiji software (58); the mean and standard deviation are reported.

Phage samples were prepared for transmission electron microscopy and imaged by previously described methods using uranyl acetate as a background stain (57) at the University of Alberta Advanced Microscopy Facility. Virion measurements were performed using Fiji software (58) from 44 phage particles; the mean and standard deviation are reported.

The host range for Kapi1 was determined by growing strains of interest overnight, and then 50 μL of overnight culture was added to 3.5 mL soft agar and poured onto an LB plate. Once solidified, Kapi1 lysate was serially diluted and spotted onto each strain. In parallel, a whole-plate overlay was prepared as described above, using 300 μL undiluted phage lysate and 50 μL overnight culture. The following day, plates were scored for presence or absence of plaques, with KP7 included as a positive control. The whole-plate overlays were collected as above for each strain tested. These “trained” Kapi1 lysates were serially diluted and spotted back onto the same strain to see if the Kapi1 host range could be expanded by extended incubation with a particular host compared to the first round of spotting.

Genome sequencing and PCR. Pure cultures were grown by streaking from glycerol cryostocks and then picking single colonies and growing overnight. DNA was extracted from overnight cultures using the Lucigen MasterPure Complete DNA and RNA purification kit, and the concentration and quality of genomic DNA (gDNA) was checked using the NanoDrop 2000c. Library preparation and whole-genome

sequencing were performed by the Microbial Genome Sequencing Centre (MiGS, Pittsburgh, PA). Libraries were prepared with the Illumina Nextera kit and sequenced using the NextSeq 550 platform.

PCR was performed using *Taq* polymerase (Invitrogen) following the manufacturer's directions; a single colony was suspended in 20 μ L nuclease-free water, and 5 μ L of this suspension was used per 50 μ L reaction mixture. Phage DNA was extracted via phenol-chloroform extraction (<https://cpt.tamu.edu/phage-links/phage-protocols/>), and 1 to 5 μ L of phage DNA was used per 50 μ L reaction. PCR products were checked by running 10 μ L on a 2% agarose gel and staining with ethidium bromide. All primers used in this study can be found in Table S2. Sanger sequencing was performed by the Molecular Biology Service Unit at the University of Alberta.

Genome assembly, annotation, and taxonomy. Paired-end reads of 2×150 bp received from MiGS were uploaded to the public server at usegalaxy.org (59). Galaxy, and all tools therein, was used for bacterial genome assembly, annotation, and analysis as follows. Illumina adapters and low-quality reads were trimmed using Trim Galore! (60). Reads were then checked for quality using FastQC (61) and MultiQC (62). Trimmed reads were *de novo* assembled using Unicycler (63), functioning as a SPAdes (64) optimizer, as no long-read data were generated. Quality of assemblies was assessed using Quast (65), and bacterial genomes were then annotated using Prokka (66, 67). SnapGene software (Insightful Science; <https://www.snapgene.com/>) was used for genome visualization, creating genome maps, and designing primers.

The Kapi1 genome was manually annotated using previously described methods (68), slightly modified. This method uses a rigorous approach to score CDSs based on various parameters; low-scoring CDSs are then discarded, and the remaining CDSs are analyzed to determine their correct start codon, again based on a scoring system. Briefly, the prophage genome was run through three auto-annotation programs, GenemarkS (69), Glimmer3 (70) at CPT Phage Galaxy public server (<https://cpt.tamu.edu/galaxy-pub>), and Prokka (66) at <https://usegalaxy.org/> (67). The coding potential for each putative CDS was determined using GenemarkS coding potential graph (69). Putative CDSs were then searched against NCBI's nonredundant protein database using BLASTp (20) and scored based on whether they had significantly similar hits (as determined by the E value, using a cutoff of e^{-10}) and whether those hits were known proteins or hypotheticals. Each CDS was scored based on the length of overlap neighboring CDSs, as extremely long overlaps are unlikely, while short overlaps of 1, 4, or 8 bp are more favorable, as these suggest organization into an operon. Finally, CDSs were scored based on the length of the open reading frame (ORF), where extremely short CDSs are penalized the most heavily. Low-scoring CDSs were discarded prior to start codon identification. Start codons for each CDS were scored in a similar manner, using, again, the coding potential graph from GenemarkS (69), the number of auto-annotation programs that selected the start codon, sequence similarity matches in NCBI, and length of the ORF. These parameters are listed in order of most important to least and were used to select the most likely start codon for each CDS. CD-Search (71) was also performed for all CDSs to assist with functional assignment.

Taxonomic evaluation was performed using vContact2 v9.8 (22) through the CyVerse platform (<https://www.cyverse.org/>). The analysis was run with the default parameters, using NCBI Bacterial and Archaeal Viral RefSeq V85 (with ICTV and NCBI taxonomy) as the reference database. The resulting network was visualized using Cytoscape (72). Duplicated edges were removed from the network (edges represent connections between two nodes, in this case, viruses), and only first neighbors to Kapi1 were kept (nodes that have a direct connection to the Kapi1 node). An edge-weighted, spring-embedded layout was used so that nodes that are more closely related appear closer together spatially, and edges were weighted so that stronger connections (i.e., more sequence similarity between two viruses) appear darker and thicker.

Lipopolysaccharide profiling. The general structure of LPS was analyzed by profiling LPS extracts on SDS-PAGE with silver staining. LPS was extracted using a modified proteinase K microdigestion protocol (73) as follows. Bacterial strains of interest were grown overnight, and then 1 mL of this culture was washed twice with phosphate-buffered saline (PBS), resuspended to a final optical density at 600 nm (OD_{600}) of 2.0 in PBS, and pelleted. Cells were resuspended in 50 μ L lysis buffer (2% SDS, 4% 2-mercaptoethanol, 10% glycerol, 1 M Tris, pH 6.8, and bromophenol blue to a deep blue color) and incubated at 95°C for 10 min to lyse cells. The whole-cell lysate was cooled to room temperature, and then 10 μ L of 2.5 mg/mL proteinase K (20 mg/mL stock solution was diluted in lysis buffer first) was added and incubated at 56°C for 1 h. Standard polyacrylamide gels were prepared with 12% acrylamide (19:1 acrylamide/bisacrylamide) (74), and 1 to 5 μ L of proteinase K-treated whole-cell lysate (LPS extract) was loaded per well and run at 80 V in Tris-glycine running buffer (25 mM Tris, 200 mM glycine, and 0.1% SDS) until the dye front nearly reached the bottom of the gel. Silver staining was performed as previously described (75) and imaged on a clear petri dish using an iPhone camera.

To determine if Kapi1 is capable of degrading LPS, LPS was extracted from cultures of KP7 (nonlysogenic for Kapi1) and MP13 Kapi1 lysogens using a phenol extraction method adapted from Davis and Goldberg (76); purified KP7 LPS was then incubated with Kapi1 and compared to the untreated controls. The phenol extraction was used in place of proteinase K digestion (as above), as Kapi1 was not viable in the lysis buffer, even after inactivation of proteinase K at high temperatures (data not shown). Briefly, KP7 and MP13 were grown overnight, and cultures were pelleted and washed in PBS and then resuspended in 1.5 mL PBS to give a final OD_{600} of 2.0. Cells were pelleted and resuspended in 200 μ L Laemmli buffer (50 mM Tris-HCl, pH 6.8, 4% SDS, 10% glycerol, 0.1% bromophenol blue, and 5% β -mercaptoethanol) and then boiled for 15 min to lyse cells. Once cool, DNase I and RNase A were added to cell lysates at 37°C for 10 min. Proteinase K was then added, and lysates were incubated at 55°C overnight. The following day, 200 μ L Tris-saturated phenol was added to lysates and then vortexed for 10 s

before incubating at 65°C for 15 min. Once cool, samples were centrifuged at 14,000 rpm for 10 min at 4°C, and the upper phase was transferred to a new tube. We added 2.5 (vol/vol) ethanol to precipitate LPS, and then it was centrifuged at 15,000 rpm for 20 min. Supernatant was discarded, and pellets were air-dried and then resuspended in 50 μ L nuclease-free water. Kapi1 was added to KP7 LPS at a multiplicity of infection ([MOI] of 10 (assuming that 1.5 mL of OD₆₀₀ 2.0 culture was concentrated into 50 μ L) and incubated at 37°C without shaking for 30 min. Phage-treated and untreated KP7 LPS, along with MP13 untreated LPS were run on SDS-PAGE and silver stained, as above, using 15 μ L of LPS extract, as this extraction method produced a lower yield). A portion of the phage-treated samples was serially diluted and spotted onto a KP7 soft-agar overlay to ensure that phage particles remained viable after incubation with LPS (data not shown).

Generation of mutants. Spontaneous Kapi1-resistant mutants were isolated by spotting Kapi1 onto a soft-agar overlay prepared with KP7. The following day, six colonies that grew within the cleared phage spots were picked and restreaked onto LB. The following day, these colonies were screened for lysogeny with Kapi1 using PCR with primers that span the phage-genome junction. Two colonies that did not produce phage-genome bands were grown overnight, and then the supernatant was filter sterilized and spotted onto a soft-agar overlay prepared with KP7. The absence of plaques on KP7 confirmed that these two mutants are not Kapi1 lysogens. To identify which mutations were responsible for the Kapi1-resistant phenotype, each colony was sent for whole-genome sequencing at MiGS, as above. SNPs were identified using BreSeq (77) and snippy (78) through Galaxy (59), using the KP7 genome as a reference.

KP7 Δ *waaF::kan* and MP13 Δ *recA::kan* mutants were constructed via P1 transduction, as previously described (79, 80), using the corresponding Keio collection mutant (81) as a donor. The previously described lambda Red system (82) was used to generate KP7 Δ *waaL::kan*. Once sequencing confirmed the correct mutation in *waaL*, P1 transduction was used (as above) to move these mutations into a fresh KP7 background to avoid the possibility of any off-site mutations acquired during construction. Putative seroconversion genes were deleted via allelic exchange, as previously described (83).

Efficiency of lysogeny, phage and cell counts, prophage stability, and luminescent reporter assays. Efficiency of lysogeny was determined by infecting KP7 and KP7 Δ *attB::kan* with Kapi1 at a multiplicity of infection of 10 at 37°C for 30 min and then washing and plating out surviving cells. The following day, survivor colonies were screened by colony PCR using primers that span the prophage_1 left junction (chromosome_1 left, prophage_1 left primers; Table S2) to look for integration of Kapi1 at the putative attB site. The same set of colonies was also grown overnight in liquid culture. Overnight cultures were then assayed for lysogeny by spotting the culture supernatant onto a soft-agar overlay prepared with KP7; the supernatants of Kapi1 lysogens produce plaques on KP7.

To monitor the CFU and PFU in cultures of MP13 Kapi1 lysogens over time, three colonies of MP13 and three colonies of KP7 (nonlysogenic control) were picked and grown overnight. The next day, cultures were adjusted to an OD₆₀₀ of 1.0 to ensure equal cell numbers and then subcultured 1:100 into LB, LB with 0.5 ng/ μ L mitomycin C, LB mixed 50:50 with simulated intestinal fluid (SIF; 6.8 g KH₂PO₄, 1.25 g pancreatin, 3 g bile salts in 1 L distilled water [dH₂O], pH adjusted to 7 [50]), or LB mixed 50:50 with simulated gastric fluid (SGF; 2 g/L NaCl, 3.2 g/L porcine mucosa pepsin, pH adjusted to 3.5 [50]). After 24 h incubation, an aliquot was taken from each culture. Cells were spun down, washed in PBS (137 mM NaCl, 2.7 mM KCl, 10 mM Na₂HPO₄, and 1.8 mM KH₂PO₄), serially diluted, plated onto LB, and grown overnight to enumerate the number of cells in the culture. In parallel, the culture supernatants (containing phage) were serially diluted, spotted onto KP121 soft-agar overlays, and incubated overnight at 30°C to enumerate the number of phage particles in the culture. KP121 was used to enumerate phages, as this strain has a much lower efficiency of lysogeny with Kapi1 than WT KP7, allowing for more accurate enumeration.

Prophage stability was assayed by serially propagating cultures of Kapi1 lysogens. MP13 cultures were grown in biological triplicates (three independent colonies) in either LB, LB mixed 50:50 with SGF, LB mixed 50:50 with SIF, or LB with 0.5 ng/ μ L mitomycin C for 24 h and then subcultured into fresh media and grown for another 24 h. After a total of 48 h incubation (1 passage), cells were spun down and washed twice in PBS, serially diluted, plated on LB, and grown overnight to get individual colonies. Using velvet squares, colonies were replicated onto an LB plate spread with 50 μ L of an overnight culture of KP7 to screen for lysogens (84). This replica-plating technique results in two distinct phenotypes: colonies that produce a zone of clearing in the KP7 lawn are scored as lysogens, and colonies without a zone of clearing are scored as nonlysogenic (see Fig. S5 for examples and experimental verification of these phenotypes). The relative loss of Kapi1 lysogens in the culture was calculated by dividing the nonlysogenic CFU/mL by the total CFU/mL.

Luminescent reporters were constructed by cloning the *Ci* promoter region into the luminescent reporter plasmid pNLP10 (52) via standard PCR cloning. Kapi1 lysogens carrying pNLP10 *Ci-lux* were grown overnight in biological triplicate in LB with kanamycin (Kan). The next day, each overnight culture was subcultured 1:50 into LB plus Kan in 4 replicates (one for each medium type) so that each medium type assayed contained the same 3 biological replicates. After 1.5 h growth, cultures were spun down for 5 min at 4,000 rpm. The supernatant was poured off, and cells were resuspended in 2 mL of either LB, 50% LB-50% SGF, 50% LB-50% SIF, or LB plus 0.5 ng/ μ L mitomycin C. To measure luminescence, 100 μ L of culture was aliquoted into a sterile black 96-well plate, then luminescence and absorbance at 600 nm were measured using the Victor X3 2020 multilabel plate reader (PerkinElmer). Luminescence (counts per second, CPS) was divided by bacterial optical density (OD₆₀₀) to account for variations in growth, and the average of 3 biological replicates was plotted, with the standard deviation shown as error bars. The experiment was repeated 3 times.

Bacterial growth curves and competitive assays. Growth curves were performed by growing each strain of interest overnight in biological triplicate in LB. The following day, cultures were adjusted to an optical density of 1.0 in PBS. These adjusted cultures were then inoculated 1:100 into either LB or SIF in a standard 96-well plate. Plates were incubated in the Epoch 2 microplate reader (Biotek, USA) at 37°C with agitation; the OD₆₀₀ was measured every 30 min for 12 h.

In vitro competitive assays were performed by growing KP7 and MP13 overnight cultures in biological triplicate. Each culture was standardized to an OD₆₀₀ of 1.0 in PBS to ensure approximately equal cell numbers, and then 10 μL of KP7 and 10 μL MP13 were subcultured into 2 mL of either LB or SIF. Immediately, cocultures were briefly vortexed, and 100 μL of the culture was aliquoted; then, cocultures were incubated at 37°C at 225 rpm for 24 h. To enumerate the starting cell counts of each strain, samples from cocultures were serially diluted 10-fold in PBS, and then 10 μL of each dilution was plated onto LB containing 15 μg/mL tetracycline using the track dilution method; once dry, plates were incubated overnight at 30°C. Plates were imaged using the ChemiDoc system, using DyLight 550 for visualization of *mcherry* and StarBright B520 for visualization of *gfpmut3.1*. Notably, although cultures were standardized to equal optical density, the starting inoculum of KP7 was much higher than MP13. We hypothesize that this is due to the demonstrated spontaneous induction of Kapi1; the resulting cell lysis in a subset of the MP13 population could result in more cellular debris and, thus, a lower number of viable cells at the same optical density measurement. Every 24 h, cocultures were subcultured 1:100 into fresh media, and again, 100 μL of the mature culture was sampled to perform cell counts as above.

In vivo studies were performed using mature adult C57BL/6J male mice kept in the animal facility at the University of Alberta. Mice not harboring coliforms, as confirmed by plating on MacConkey agar (BD, Sparks, MD), were housed on aspen wood chip bedding materials in sterilized filter-topped IsoCages with nestlets, mouse huts, and nesting materials as enhancements. The room environment was controlled for temperature (20 to 22°C), relative humidity (40%), and light cycle (12 h light and 12 h darkness). Mice were given *ad libitum* access to water and a standard chow diet, and cages were handled in a biosafety cabinet under specific-pathogen-free conditions. Animals were randomly grouped into 4 to 5 mice per cage by a blinded lab animal technician. Cages were allocated into 3 treatments, colonization with KP7, colonization with MP13, and competitive colonization with a mixture of KP7 and MP13. KP7 and MP13 were cultivated in 10 mL of LB medium (Fisher Scientific, Nepean, Ontario, Canada) at 37°C for 16 h. Each mouse received 0.1 mL of culture medium containing approximately 1.0×10^7 CFU of *E. coli* cells by oral gavage. Body weights were recorded, and fecal samples were collected at 0, 7, 14, and 28 days postinfection (dpi). Enumeration of *E. coli* was conducted by serial dilutions of fecal samples plated on MacConkey agar, and total CFU per gram of feces were then calculated. For competitive colonization, MacConkey plates were replica plated onto LB plus tetracycline (Tet) and imaged as above. The protocols employed were approved by the University of Alberta's Animal Care Committee and in accordance with the guidelines of the Canadian Council on the Use of Laboratory Animals.

Statistics and data visualization. The Shapiro-Wilk test was used to check the normality of data distribution, and the log transformation or arcsine transformation was applied to address skewed data. Student's *t* test or one-way analysis of variance (ANOVA) with Tukey's *post hoc* test was performed accordingly. Data were presented as mean ± standard deviation (SD). A *P* value below 0.05 was considered statistically significant. Unless otherwise specified, statistical analysis was performed using either Microsoft Excel or GraphPad Prism 7 (85), and graphs were generated in Microsoft Excel.

Data availability. The genome of Kapi1 can be accessed from NCBI GenBank (accession no. [MT813197](#)).

SUPPLEMENTAL MATERIAL

Supplemental material is available online only.

FIG S1, TIF file, 2.1 MB.

FIG S2, TIF file, 1.3 MB.

FIG S3, TIF file, 2.6 MB.

FIG S4, TIF file, 1.6 MB.

FIG S5, TIF file, 2.5 MB.

TABLE S1, DOCX file, 0.02 MB.

TABLE S2, DOCX file, 0.01 MB.

TABLE S3, DOCX file, 0.03 MB.

ACKNOWLEDGMENTS

We thank Arlene Oatway from the University of Alberta Advanced Microscopy Facility for assistance with transmission electron microscopy; the University of Alberta Molecular Biology Facility for assistance with Sanger sequencing; the Microbial Genome Sequencing Centre for assistance with whole-genome sequencing; Mark Goulian for critical reading of the manuscript and for strains MP1, MP7, and MP13; Jaclyn McCutcheon for advice on phage isolation and preliminary characterization; Brent Weber for advice on identification of the integration site; Ashley Gilliland for thoughtful discussion of results and data analysis; and Stephanie Tollenaar for assistance with animal work.

This research was supported by operating grants from The National Sciences and Engineering Research Council (NSERC) and The Canadian Institutes of Health Research (CIHR), and a project grant from the AMR-One Health Consortium, funded by the Major Innovation Fund program of the Ministry of Jobs, Economy and Innovation, Government of Alberta, to T.R. B.P.W. is supported by the Canada Research Chairs program. K.P. was supported by an NSERC Alexander Graham Bell Canada Graduate Scholarship-Master's, Walter H Johns Graduate Fellowship, University of Alberta Science Graduate Scholarship, and Susan Eberlein Graduate Scholarship in Genetics.

REFERENCES

- Tenaillon O, Skurnik D, Picard B, Denamur E. 2010. The population genetics of commensal *Escherichia coli*. *Nat Rev Microbiol* 8:207–217. <https://doi.org/10.1038/nrmicro2298>.
- Howard-Varona C, Hargreaves KR, Abedon ST, Sullivan MB. 2017. Lysogeny in nature: mechanisms, impact and ecology of temperate phages. *ISME J* 11:1511–1520. <https://doi.org/10.1038/ismej.2017.16>.
- Touchon M, Bernheim A, Rocha EPC. 2016. Genetic and life-history traits associated with the distribution of prophages in bacteria. *ISME J* 10:2744–2754. <https://doi.org/10.1038/ismej.2016.47>.
- Kim MS, Bae JW. 2018. Lysogeny is prevalent and widely distributed in the murine gut microbiota. *ISME J* 12:1127–1141. <https://doi.org/10.1038/s41396-018-0061-9>.
- Hsu BB, Gibson TE, Yeliseyev V, Liu Q, Lyon L, Bry L, Silver PA, Gerber GK. 2019. Dynamic modulation of the gut microbiota and metabolome by bacteriophages in a mouse model. *Cell Host Microbe* 25:803–814.e5. <https://doi.org/10.1016/j.chom.2019.05.001>.
- Fraão N, Sousa A, Lässig M, Gordo I. 2019. Horizontal gene transfer overrides mutation in *Escherichia coli* colonizing the mammalian gut. *Proc Natl Acad Sci U S A* 116:17906–17915. <https://doi.org/10.1073/pnas.1906958116>.
- Davies EV, Winstanley C, Fothergill JL, James CE. 2016. The role of temperate bacteriophages in bacterial infection. *FEMS Microbiol Lett* 363:fnw015. <https://doi.org/10.1093/femsle/fnw015>.
- Van Belleghem JD, Dąbrowska K, Vaneechoutte M, Barr JJ, Bollyky PL. 2019. Interactions between bacteriophage, bacteria, and the mammalian immune system. *Viruses* 11:10. <https://doi.org/10.3390/v11010010>.
- Allison GE, Verma NK. 2000. Serotype-converting bacteriophages and O-antigen modification in *Shigella flexneri*. *Trends Microbiol* 8:17–22. [https://doi.org/10.1016/s0966-842x\(99\)01646-7](https://doi.org/10.1016/s0966-842x(99)01646-7).
- Guest RL, Rutherford ST, Silhavy TJ. 2020. Border control: regulating LPS biogenesis. *Trends Microbiol* 29:334–345. <https://doi.org/10.1016/j.tim.2020.09.008>.
- Lasaro M, Liu Z, Bishar R, Kelly K, Chattopadhyay S, Paul S, Sokurenko E, Zhu J, Goulian M. 2014. *Escherichia coli* isolate for studying colonization of the mouse intestine and its application to two-component signaling knockouts. *J Bacteriol* 196:1723–1732. <https://doi.org/10.1128/JB.01296-13>.
- Arndt D, Grant JR, Marcu A, Sajed T, Pon A, Liang Y, Wishart DS. 2016. PHASTER: a better, faster version of the PHAST phage search tool. *Nucleic Acids Res* 44:W16–W21. <https://doi.org/10.1093/nar/gkw387>.
- Zhou Y, Liang Y, Lynch KH, Dennis JJ, Wishart DS. 2011. PHAST: a fast phage search tool. *Nucleic Acids Res* 39:347–352. <https://doi.org/10.1093/nar/gkr485>.
- Schoch CL, Ciufo S, Domrachev M, Hottton CL, Kannan S, Khovanskaya R, Leipe D, McVeigh R, O'Neill K, Robbertse B, Sharma S, Soussov V, Sullivan JP, Sun L, Turner S, Karsch-Mizrachi I. 2020. NCBI Taxonomy: a comprehensive update on curation, resources and tools. *Database* 2020:baaa062. <https://doi.org/10.1093/database/baaa062>.
- Ju T, Shoblak Y, Gao Y, Yang K, Fuhse J, Finlay B, Wing So Y, Stothard P, Willing BP. 2017. Initial gut microbial composition as a key factor driving host response to antibiotic treatment, as exemplified by the presence or absence of commensal *Escherichia coli*. *Appl Environ Microbiol* 83:e01107-17. <https://doi.org/10.1128/AEM.01107-17>.
- Hull RA, Gill RE, Hsu P, Minshew BH, Falkow S. 1981. Construction and expression of recombinant plasmids encoding type 1 or D-mannose-resistant pili from a urinary tract infection *Escherichia coli* isolate. *Infect Immun* 33:933–938. <https://doi.org/10.1128/iai.33.3.933-938.1981>.
- Iguchi A, Thomson NR, Ogura Y, Saunders D, Ooka T, Henderson IR, Harris D, Asadulghani M, Kurokawa K, Dean P, Kenny B, Quail MA, Thurston S, Dougan G, Hayashi T, Parkhill J, Frankel G. 2009. Complete genome sequence and comparative genome analysis of enteropathogenic *Escherichia coli* O127:H6 strain E2348/69. *J Bacteriol* 191:347–354. <https://doi.org/10.1128/JB.01238-08>.
- Nissle A. 1918. Die antagonistische Behandlung chronischer Darmstörungen mit Colibakterien. *Med Klin* 29–30.
- Mathieu A, Dion M, Deng L, Tremblay D, Moncaut E, Shah SA, Stokholm J, Krogfelt KA, Schjörriing S, Bisgaard H, Nielsen DS, Moineau S, Petit MA. 2020. Virulent coliphages in 1-year-old children fecal samples are fewer, but more infectious than temperate coliphages. *Nat Commun* 11:378. <https://doi.org/10.1038/s41467-019-14042-z>.
- Altschul SF, Gish W, Miller W, Myers EW, Lipman DJ. 1990. Basic local alignment search tool. *J Mol Biol* 215:403–410. [https://doi.org/10.1016/S0022-2836\(05\)80360-2](https://doi.org/10.1016/S0022-2836(05)80360-2).
- Adriaenssens EM, Rodney Brister J. 2017. How to name and classify your phage: an informal guide. *Viruses* 9:70–79. <https://doi.org/10.3390/v9040070>.
- Bin Jang H, Bolduc B, Zablocki O, Kuhn JH, Roux S, Adriaenssens EM, Brister JR, Kropinski AM, Krupovic M, Lavigne R, Turner D, Sullivan MB. 2019. Taxonomic assignment of uncultivated prokaryotic virus genomes is enabled by gene-sharing networks. *Nat Biotechnol* 37:632–639. <https://doi.org/10.1038/s41587-019-0100-8>.
- Neal BL, Brown PK, Reeves PR. 1993. Use of *Salmonella* phage P22 for transduction in *Escherichia coli*. *J Bacteriol* 175:7115–7118. <https://doi.org/10.1128/jb.175.21.7115-7118.1993>.
- Jakhetia R, Marri A, Stähle J, Widmalm G, Verma NK. 2014. Serotype-conversion in *Shigella flexneri*: identification of a novel bacteriophage, Sf101, from a serotype 7a strain. *BMC Genomics* 15:742. <https://doi.org/10.1186/1471-2164-15-742>.
- Clark AJ, Inwood W, Cloutier T, Dhillon TS. 2001. Nucleotide sequence of coliphage HK620 and the evolution of lambdoid phages. *J Mol Biol* 311:657–679. <https://doi.org/10.1006/jmbi.2001.4868>.
- Nakata K, Koh MM, Tsuchido T, Matsumura Y. 2010. All genomic mutations in the antimicrobial surfactant-resistant mutant, *Escherichia coli* OW66, are involved in cell resistance to surfactant. *Appl Microbiol Biotechnol* 87:1895–1905. <https://doi.org/10.1007/s00253-010-2638-8>.
- McFall E, Heincz M. 1983. Identification and control of synthesis of the dsdC activator protein. *J Bacteriol* 153:872–877. <https://doi.org/10.1128/jb.153.2.872-877.1983>.
- Moritz RL, Welch RA. 2006. The *Escherichia coli* argW-dsdCXA genetic island is highly variable, and *E. coli* K1 strains commonly possess two copies of dsdCXA. *J Clin Microbiol* 44:4038–4048. <https://doi.org/10.1128/JCM.01172-06>.
- Reiter W-D, Palm P, Yeats S. 1989. Transfer RNA genes frequently serve as integration sites for prokaryotic genetic elements. *Nucleic Acids Res* 17:1907–1914. <https://doi.org/10.1093/nar/17.5.1907>.
- Casjens S, Winn-Stapley DA, Gilcrease EB, Morona R, Kühlewein C, Chua JEH, Manning PA, Inwood W, Clark AJ. 2004. The chromosome of *Shigella flexneri* bacteriophage Sf6: complete nucleotide sequence, genetic mosaicism, and DNA packaging. *J Mol Biol* 339:379–394. <https://doi.org/10.1016/j.jmb.2004.03.068>.
- Panis G, Méjean V, Ansaldi M. 2007. Control and regulation of KpIE1 prophage site-specific recombination: a new recombination module analyzed. *J Biol Chem* 282:21798–21809. <https://doi.org/10.1074/jbc.M701827200>.
- Silva JB, Storms Z, Sauvageau D. 2016. Host receptors for bacteriophage adsorption. *FEMS Microbiol Lett* 363:fnw002. <https://doi.org/10.1093/femsle/fnw002>.
- Dhillon TS, Poon APW, Chan D, Clark AJ. 1998. General transducing phages like *Salmonella* phage P22 isolated using a smooth strain of *Escherichia coli* as host. *FEMS Microbiol Lett* 161:129–133. <https://doi.org/10.1111/j.1574-6968.1998.tb12938.x>.

34. Samuel G, Reeves P. 2003. Biosynthesis of O-antigens: genes and pathways involved in nucleotide sugar precursor synthesis and O-antigen assembly. *Carbohydr Res* 338:2503–2519. <https://doi.org/10.1016/j.carres.2003.07.009>.
35. Heinrichs DE, Monteiro MA, Perry MB, Whitfield C. 1998. The assembly system for the lipopolysaccharide R2 core-type of *Escherichia coli* is a hybrid of those found in *Escherichia coli* K-12 and *Salmonella enterica*. Structure and function of the R2 WaaK and WaaL homologs. *J Biol Chem* 273: 8849–8859. <https://doi.org/10.1074/jbc.273.15.8849>.
36. Gronow S, Brabetz W, Brade H. 2000. Comparative functional characterization in vitro of heptosyltransferase I (WaaC) and II (WaaF) from *Escherichia coli*. *Eur J Biochem* 267:6602–6611. <https://doi.org/10.1046/j.1432-1327.2000.01754.x>.
37. Wang Z, Wang J, Ren G, Li Y, Wang X. 2016. Deletion of the genes waaC, waaF, or waaG in *Escherichia coli* W3110 disables the flagella biosynthesis. *J Basic Microbiol* 56:1021–1035. <https://doi.org/10.1002/jobm.201600065>.
38. Abedon ST. 2018. Detection of bacteriophages: phage plaques, p 1–32. *In* Harper D, Abedon S, Burrows B, McConville M (ed), *Bacteriophages*. Springer, Cham, Switzerland. https://doi.org/10.1007/978-3-319-40598-8_16-1.
39. Verma NK, Brandt JM, Verma DJ, Lindberg AA. 1991. Molecular characterization of the O-acetyl transferase gene of converting bacteriophage SF6 that adds group antigen 6 to *Shigella flexneri*. *Mol Microbiol* 5:71–75. <https://doi.org/10.1111/j.1365-2958.2001.tb01827.x>.
40. Vander Byl C, Kropinski AM. 2000. Sequence of the genome of *Salmonella* bacteriophage P22. *J Bacteriol* 182:6472–6481. <https://doi.org/10.1128/JB.182.22.6472-6481.2000>.
41. Amann E, Ochs B, Abel KJ. 1988. Tightly regulated tac promoter vectors useful for the expression of unfused and fused proteins in *Escherichia coli*. *Gene* 69:301–315. [https://doi.org/10.1016/0378-1119\(88\)90440-4](https://doi.org/10.1016/0378-1119(88)90440-4).
42. Newton GJ, Daniels C, Burrows LL, Kropinski AM, Clarke AJ, Lam JS. 2001. Three-component-mediated serotype conversion in *Pseudomonas aeruginosa* by bacteriophage D3. *Mol Microbiol* 39:1237–1247. <https://doi.org/10.1111/j.1365-2958.2001.02311.x>.
43. Norrander J, Kempe T, Messing J. 1983. Construction of improved M13 vectors using oligodeoxynucleotide-directed mutagenesis. *Gene* 26: 101–106. [https://doi.org/10.1016/0378-1119\(83\)90040-9](https://doi.org/10.1016/0378-1119(83)90040-9).
44. Ferrières L, Hémeury G, Nham T, Guéroult AM, Mazel D, Beloin C, Ghigo JM. 2010. Silent mischief: bacteriophage Mu insertions contaminate products of *Escherichia coli* random mutagenesis performed using suicidal transposon delivery plasmids mobilized by broad-host-range RP4 conjugative machinery. *J Bacteriol* 192:6418–6427. <https://doi.org/10.1128/JB.00621-10>.
45. Edwards RA, Keller LH, Schifferli DM. 1998. Improved allelic exchange vectors and their use to analyze 987P fimbria gene expression. *Gene* 207: 149–157. [https://doi.org/10.1016/S0378-1119\(97\)00619-7](https://doi.org/10.1016/S0378-1119(97)00619-7).
46. Broecker NK, Barbirz S. 2017. Not a barrier but a key: how bacteriophages exploit host's O-antigen as an essential receptor to initiate infection. *Mol Microbiol* 105:353–357. <https://doi.org/10.1111/mmi.13729>.
47. Roberts JW, Roberts CW, Craig NL. 1978. *Escherichia coli* recA gene product inactivates phage lambda repressor. *Proc Natl Acad Sci U S A* 75: 4714–4718. <https://doi.org/10.1073/pnas.75.10.4714>.
48. Little JW, Edmiston SH, Pacelli LZ, Mount DW. 1980. Cleavage of the *Escherichia coli* lexA protein by the recA protease. *Proc Natl Acad Sci U S A* 77: 3225–3229. <https://doi.org/10.1073/pnas.77.6.3225>.
49. Baharoglu Z, Mazel D. 2014. SOS, the formidable strategy of bacteria against aggressions. *FEMS Microbiol Rev* 38:1126–1145. <https://doi.org/10.1111/1574-6976.12077>.
50. Millette M, Nguyen A, Amine KM, Lacroix M. 2013. Gastrointestinal survival of bacteria in commercial probiotic products. *Int J Probiotics Prebiotics* 8:149–156.
51. Dodd IB, Shearwin KE, Egan JB. 2005. Revisited gene regulation in bacteriophage λ. *Curr Opin Genet Dev* 15:145–152. <https://doi.org/10.1016/j.gde.2005.02.001>.
52. Price NL, Raivio TL. 2009. Characterization of the Cpx regulon in *Escherichia coli* strain MC4100. *J Bacteriol* 191:1798–1815. <https://doi.org/10.1128/JB.00798-08>.
53. Wang X, Kim Y, Ma Q, Hong SH, Pokusaeva K, Sturino JM, Wood TK. 2010. Cryptic prophages help bacteria cope with adverse environments. *Nat Commun* 1:147. <https://doi.org/10.1038/ncomms1146>.
54. De Paepe M, Tournier L, Moncaut E, Son O, Langella P, Petit MA. 2016. Carriage of λ latent virus is costly for its bacterial host due to frequent reactivation in monoxenic mouse intestine. *PLoS Genet* 12:e1005861. <https://doi.org/10.1371/journal.pgen.1005861>.
55. Oh JH, Alexander LM, Pan M, Schueler KL, Keller MP, Attie AD, Walter J, van Pijkeren JP. 2019. Dietary fructose and microbiota-derived short-chain fatty acids promote bacteriophage production in the gut symbiont *Lactobacillus reuteri*. *Cell Host Microbe* 25:273–284. <https://doi.org/10.1016/j.chom.2018.11.016>.
56. Oh JH, Lin XB, Zhang S, Tollenaar SL, Özçam M, Dunphy C, Walter J, van Pijkeren JP. 2019. Prophages in *Lactobacillus reuteri* are associated with fitness trade-offs but can increase competitiveness in the gut ecosystem. *Appl Environ Microbiol* 86:1–22. <https://doi.org/10.1128/AEM.01922-19>.
57. Peters DL, Mccutcheon JG, Stothard P, Dennis JJ. 2019. Novel *Stenotrophomonas maltophilia* temperate phage DLP4 is capable of lysogenic conversion. *BMC Genomics* 20:300. <https://doi.org/10.1186/s12864-019-5674-5>.
58. Schindelin J, Arganda-Carreras I, Frise E, Kaynig V, Longair M, Pietzsch T, Preibisch S, Rueden C, Saalfeld S, Schmid B, Tinevez JY, White DJ, Hartenstein V, Eliceiri K, Tomancak P, Cardona A. 2012. Fiji: an open-source platform for biological-image analysis. *Nat Methods* 9:676–682. <https://doi.org/10.1038/nmeth.2019>.
59. Afgan E, Baker D, Batut B, Van Den Beek M, Bouvier D, Ech M, Chilton J, Clements D, Coraor N, Grüning BA, Guerler A, Hillman-Jackson J, Hiltemann S, Jalili V, Rasche H, Soranzo N, Goecks J, Taylor J, Nekruteno A, Blankenberg D. 2018. The Galaxy platform for accessible, reproducible and collaborative biomedical analyses: 2018 update. *Nucleic Acids Res* 46:W537–W544. <https://doi.org/10.1093/nar/gky379>.
60. Babraham Bioinformatics. 2012. Trim Galore! A wrapper tool around Cutadapt and FastQC to consistently apply quality and adapter trimming to FastQ files. https://www.bioinformatics.babraham.ac.uk/projects/trim_galore/.
61. Babraham Bioinformatics. 2010. FastQC: a quality control tool for high throughput sequence data. <http://www.bioinformatics.babraham.ac.uk/projects/fastqc/>.
62. Ewels P, Magnusson M, Lundin S, Käller M. 2016. MultiQC: summarize analysis results for multiple tools and samples in a single report. *Bioinformatics* 32:3047–3048. <https://doi.org/10.1093/bioinformatics/btw354>.
63. Wick RR, Judd LM, Gorrie CL, Holt KE. 2017. Unicycler: resolving bacterial genome assemblies from short and long sequencing reads. *PLoS Comput Biol* 13:e1005595. <https://doi.org/10.1371/journal.pcbi.1005595>.
64. Bankevich A, Nurk S, Antipov D, Gurevich AA, Dvorkin M, Kulikov AS, Lesin VM, Nikolenko SI, Pham S, Prijbelski AD, Pyshkin AV, Sirotkin AV, Vyahhi N, Tesler G, Alekseyev MA, Pevzner PA. 2012. SPAdes: a new genome assembly algorithm and its applications to single-cell sequencing. *J Comput Biol* 19:455–477. <https://doi.org/10.1089/cmb.2012.0021>.
65. Mikheenko A, Prijbelski A, Saveliev V, Antipov D, Gurevich A. 2018. Versatile genome assembly evaluation with QUAST-LG. *Bioinformatics* 34: i142–i150. <https://doi.org/10.1093/bioinformatics/bty266>.
66. Seemann T. 2014. Prokka: rapid prokaryotic genome annotation. *Bioinformatics* 30:2068–2069. <https://doi.org/10.1093/bioinformatics/btu153>.
67. Cuccuru G, Orsini M, Pinna A, Sbardellati A, Soranzo N, Travaglione A, Uva P, Zanetti G, Fotia G. 2014. Orione, a web-based framework for NGS analysis in microbiology. *Bioinformatics* 30:1928–1929. <https://doi.org/10.1093/bioinformatics/btu135>.
68. Salisbury A, Tsourkas PK. 2019. A method for improving the accuracy and efficiency of bacteriophage genome annotation. *Int J Mol Sci* 20:3391. <https://doi.org/10.3390/ijms20143391>.
69. Besemer J, Lomsadze A, Borodovsky M. 2001. GeneMarkS: a self-training method for prediction of gene starts in microbial genomes. Implications for finding sequence motifs in regulatory regions. *Nucleic Acids Res* 29: 2607–2618. <https://doi.org/10.1093/nar/29.12.2607>.
70. Delcher A, Bratke K, Powers E, Salzberg S. 2007. Identifying bacterial genes and endosymbiont DNA with Glimmer. *Bioinformatics* 23:673–679. <https://doi.org/10.1093/bioinformatics/btm009>.
71. Marchler-Bauer A, Lu S, Anderson JB, Chitsaz F, Derbyshire MK, DeWeese-Scott C, Fong JH, Geer LY, Geer RC, Gonzales NR, Gwadz M, Hurwitz DI, Jackson JD, Ke Z, Lanczycki CJ, Lu F, Marchler GH, Mullokandov M, Omelchenko MV, Robertson CL, Song JS, Thang N, Yamashita RA, Zhang D, Zhang N, Zheng C, Bryant SH. 2011. CDD: a conserved domain database for the functional annotation of proteins. *Nucleic Acids Res* 39: 225–229. <https://doi.org/10.1093/nar/gkq1189>.
72. Shannon P, Markiel A, Ozier O, Baliga NS, Wang JT, Ramage D, Amin N, Schwikowski B, Ideker T. 2003. Cytoscape: a software environment for integrated models of biomolecular interaction networks. *Genome Res* 13: 2498–2504. <https://doi.org/10.1101/gr.1239303>.
73. Hitchcock PJ. 1984. Analyses of gonococcal lipopolysaccharide in whole-cell lysates by sodium dodecyl sulfate-polyacrylamide gel electrophoresis: stable association of lipopolysaccharide with the major outer membrane protein (protein I) of *Neisseria gonorrhoeae*. *Infect Immun* 46: 202–212. <https://doi.org/10.1128/iai.46.1.202-212.1984>.

74. Kulikov EE, Golomidova AK, Prokhorov NS, Ivanov PA, Letarov AV. 2019. High-throughput LPS profiling as a tool for revealing of bacteriophage infection strategies. *Sci Rep* 9:2958. <https://doi.org/10.1038/s41598-019-39590-8>.
75. Tsai C, Frasch C. 1982. Silver stain for detecting lipopolysaccharides polyacrylamide gels. *Anal Biochem* 119:115–119. [https://doi.org/10.1016/0003-2697\(82\)90673-X](https://doi.org/10.1016/0003-2697(82)90673-X).
76. Davis MR, Goldberg JB. 2012. Purification and visualization of lipopolysaccharide from Gram-negative bacteria by hot aqueous-phenol extraction. *J Vis Exp* 28:3916. <https://doi.org/10.3791/3916>.
77. Deatherage DE, Barrick JE. 2014. Identification of mutations in laboratory evolved microbes from next-generation sequencing data using breseq. *Methods Mol Biol* 1151:115–119. https://doi.org/10.1007/978-1-4939-0554-6_12.
78. Seemann T. 2015. snippy: fast bacterial variant calling from NGS reads. <https://github.com/tseemann/snippy>.
79. Sambrook J, Russell DW. 2001. *Molecular cloning: a laboratory manual*, 3rd ed. Cold Spring Harbor Laboratory Press, Cold Spring Harbor, NY.
80. Silhavy TJ, Berman ML, Enquist LW. 1984. *Experiments with gene fusions*. Cold Spring Harbor Laboratory Press, Cold Spring Harbor, NY.
81. Baba T, Ara T, Hasegawa M, Takai Y, Okumura Y, Baba M, Datsenko KA, Tomita M, Wanner BL, Mori H. 2006. Construction of *Escherichia coli* K-12 in-frame, single-gene knockout mutants: the Keio collection. *Mol Syst Biol* 2:2006.0008. <https://doi.org/10.1038/msb4100050>.
82. Datsenko KA, Wanner BL. 2000. One-step inactivation of chromosomal genes in *Escherichia coli* K-12 using PCR products. *Proc Natl Acad Sci U S A* 97:6640–6645. <https://doi.org/10.1073/pnas.120163297>.
83. Vogt SL, Scholz R, Peng Y, Guest RL, Scott NE, Woodward SE, Foster LJ, Raivio TL, Finlay BB. 2019. Characterization of the *Citrobacter rodentium* Cpx regulon and its role in host infection. *Mol Microbiol* 111:700–716. <https://doi.org/10.1111/mmi.14182>.
84. Lederberg EM, Lederberg J. 1953. Genetic studies of lysogenicity in *Escherichia coli*. *Genetics* 38:51–64. <https://doi.org/10.1093/genetics/38.1.51>.
85. GraphPad Software. GraphPad Prism. www.graphpad.com.
86. Wintersinger JA, Wasmuth JD. 2015. Kablammo: an interactive, web-based BLAST results visualizer. *Bioinformatics* 31:1305–1306. <https://doi.org/10.1093/bioinformatics/btu808>.
87. Kropinski AM. 2009. Measurement of the rate of attachment of bacteriophage to cells. *Methods Mol Biol* 501:151–155. https://doi.org/10.1007/978-1-60327-164-6_15.